A consensus approach for estimating health risk: Application to inhalation cancer risks

Pascal Petit, Anne Maître, Dominique J. Bicout

HAL Id: hal-03364366
https://hal.univ-grenoble-alpes.fr/hal-03364366

Submitted on 9 May 2023

A consensus approach for estimating health risk: application to inhalation cancer risks

Pascal Petit[a,*], Anne Maître[a,b], Dominique J. Bicout[a,c,d,*]

[a] Grenoble Alpes University, CNRS, Grenoble INP, TIMC-IMAG (UMR 5525 CNRS - UGA), EPSP team (Environment and Health Prediction of Populations), F-38000 Grenoble, France

[b] Grenoble Alpes teaching Hospital, Occupational and Environmental Toxicology Laboratory, Biochemistry Molecular Biology and Environmental Toxicology Department, Biology and Pathology Institute, F-38000 Grenoble, France

[c] Biomathematics and Epidemiology EPSP-TIMC, VetAgro Sup, Veterinary Campus of Lyon, Marcy l'Etoile, France

[d] Laue – Langevin Institute, Theory group, Grenoble, France

[*] Corresponding authors at: Laboratoire TIMC-IMAG, Equipe EPSP, Faculté de Médecine de Grenoble, Domaine de La Merci, 38706 La Tronche Cedex, France.

E-mail address: pascal.petit@univ-grenoble-alpes.fr, dominique.bicout@univ-grenoble-alpes.fr

ABSTRACT

Conducting a risk assessment is challenging because various and contrasting risk indicators are available, which can lead to discrepancies and, sometimes, conflicting conclusions. Constructing and using a consensus risk indicator (CRI) could provide a reliable alternative that is consistent and supports direct comparisons. The goal of this study is to propose a structured and pragmatic approach for constructing a CRI distribution and demonstrate its feasibility and easy implementation when conducting risk assessments. A CRI distribution is constructed as a weighted combination of existing indicators where the weights are obtained by using the overlapping areas of an individual indicator's distribution and an aggregated reference distribution. The approach is illustrated through an assessment of human cancer risk following inhalation exposure. The CRI is constructed using eight risk indicators. The CRI distribution parameters for 199 human carcinogenic chemicals associated with inhalation exposure were determined and are presented in an interactive table. To aid the wider implementation of the CRI approach, a user-friendly and interactive web application, named InCaRisk, was created to facilitate the cancer risk estimation following inhalation exposure. Our approach could be useful for enhancing the quality of regulatory decisions and protecting human health from environmental pollutants; our approach can be applied for a given health outcome, route of exposure and exposure setting.

1. INTRODUCTION

One common task in the everyday life of a person is to make a decision based on the information at their disposal. Making a "right" decision depends on the context, experience and background of the decision maker and can become very complex when the available data do not concur or differ tremendously. This is a common issue encountered by practitioners, risk assessors and decision makers when assessing environmental health risks. In health-related fields, making a decision will have broad and profound implications, especially in regard to the prevention and protection of the health and safety of the exposed population. The controversies surrounding the use and safety of pesticides and products containing endocrine disruptors are good examples of these kinds of issues and their implications (Mesnage and Antoniou, 2017; Tarazona et al., 2017; Warner and Flaws, 2018).

Risk assessments are paramount in ensuring the protection of human health against environmental pollutants (Rotter et al., 2018). The goal of risk assessment is to decide whether a given exposure to an agent is acceptable in regard human health by empowering decision makers with valuable knowledge and insights. This is not a simple matter, especially when considering low doses and chronic exposures. Indeed, people are not exposed to a single pollutant but to a mixture of them (either simultaneously or sequentially) with evolving compositions, concentrations and interactions (cocktail effects) through different absorption pathways (oral, respiratory, cutaneous) and different evolving

---

Abbreviations: α: scaling constant related to the exposure duration and the reference value of a pollutant (e.g., unit risk); γ: stiffness factor; λ_k: eigenvalues associated to the (normalized to one) eigenvectors v_k of the matrix O; μ_{log}: natural logarithm mean; v_k: eigenvectors of the matrix O; ω_i: weight attributed to each indicator for the consensual risk indicator; σ: the standard deviation of the d_i; σ_{log}: natural logarithm standard deviation; A: total overlap between $g_r(z)$ and all $f_i(z)$; A_{max}: total overlap between all z_i; AT: averaging time; b: offset from the reference distribution $g_r(z)$; BaP: benzo[a]pyrene; BW: average body weight of an adult (70 kg); C: exposure concentration of a chemical; CDF: cumulative distribution function; CRI: consensual risk indicator; CSF: inhalation cancer slope factor; d_i: overlap distance between the indicator "i" and the reference distribution; ED: exposure duration; EF: exposure frequency; ET: exposure time; $f_i(z)$: random variable of distribution; $g(z)$: consensual distribution, resulting from the aggregation of the n indicator distributions; GM: geometric mean; $g_r(z)$: reference distribution; GSD: geometric standard deviation; i: risk indicator; $ILCR$: incremental lifetime cancer risk; IR: average inhalation rate of an adult (20 m³/day); IUR: inhalation unit risk; MRL: Minimal Risk Level; n: number of indicators; O: overlap matrix; $OEHHA$: California Office of Environmental Health Hazard Assessment; O_{ij}: overlap between two distribution functions $f_i(z)$ and $f_j(z)$; $P(\cdots)$: distribution of C; PDF: probability density function; r: risk of occurrence; R_c: consensual risk; R_i: risk of a given indicator; s: statistics (i.e. mean, median, 95th percentile…); s_r: statistics associated to the reference distribution $g_r(z)$; z_i: factor describing the characteristics of the exposure taken into account in the indicator "i" to estimate the risk.

settings/environments (indoor or urban exposure, occupational settings) during any life stage (Backhaus and Faust, 2012; Williams et al., 2012).

Risk assessment is typically performed for a single pollutant, as there is no approach for assessing the risk of exposures to a mixture of pollutants. Exposure conditions, mode of actions and health outcomes vary greatly depending on the type and number of agents considered, and most toxicological data are derived from experimental animal studies. As a result, the nature of all risk issues cannot be considered similar in nature, leading to the implementation of different strategies for tackling the existing risk problems (Lebret, 2016). One of the major challenges encountered when conducting a risk assessment arises when choosing of the most relevant approach and risk indicator. Various contrasting risk indicators exist and differ from one another in the relationships between the exposure condition and the risk. These indicators have been developed by different organizations under various jurisdictions and regulatory settings in several countries, which leads to discrepancies and occasionally conflicting conclusions (Abt et al., 2010; Chartres et al., 2019; Slob et al., 2014). This might be explained by the fact that there is, to our knowledge, no international guidelines, recommendation or accepted gold standard regarding the best choice and conditions for using these indicators (Chartres et al., 2019). In addition, the determination, number and values of the established reference indexes differ from one organization to another. These observations emphasize the differences and difficulties in decision making that emanate from these inconsistencies and the lack of a standardized method. A standardized risk assessment-based approach for comparative risk assessment is thus needed to provide consistency and support direct comparisons between studies and countries, as well as to allow for the ability to assess changes in risk and to weigh the benefits of risk management versus the costs. Such an approach could enhance the quality of regulatory decisions and protect human health from environmental pollutants that are mainly emitted by anthropogenic sources such as hazardous materials. Constructing and using a consensus risk indicator (CRI) could be a reliable alternative in addressing this issue. Such a CRI would aggregate the outputs of several available indicators for the same route of exposure and health outcome/event (e.g., inhalation cancer risk) to produce a single combined probability distribution and could be more useful and informative for conducting a health risk assessment than using only one single indicator.

This work aims to propose a clearly structured and pragmatic approach for creating a consensus distribution that can be used for conducting risk assessments. To that end, the overlapping area between an individual indicator's distribution and an aggregated distribution is used to determine the weight of the considered indicator. The proposed approach is illustrated by applying it to human inhalation cancer risk assessment and creating an interactive table and an interactive web application, called InCaRisk, to make navigation and use more user friendly by facilitating the understanding, manipulation and extraction of data.

The paper is organized as follows: i) the general approach for constructing a CRI, and the application of a CRI to inhalation cancer risk, ii) the description and characterization of existing inhalation risk indicators, iii) the construction of a CRI for inhalation cancer risk and iv) an illustration of the use of the constructed CRI.

2. MATERIALS AND METHODS

2.1 Construction of a consensus risk indicator (CRI)

In general, consider an event (for example, the occurrence of a disease) for which we want to calculate risk r of occurrence. To do this, we have n independent indicators, each giving a risk r_i of occurrence for the same event and route of exposure. To maintain generality, we consider that risk r_i is a random variable of (normalized to unity) distribution $R_i(r)$. The question that concerns us is how to calculate and construct a consensus distribution, $R_c(r)$, with $R_i(r)$ $(i = 1,2,\cdots,n)$ distributions of n indicators. First, it is assumed that all n indicators hold and bring an element of truth that is included in the consensus analysis. In the absence of indications, the simplest way to construct a consensus distribution of risks, $R_c(r)$, with $R_i(r)$ is to linearly combine all $R_i(r)$ as follows (Eq. 1):

$$R_c(r) = \sum_{i=1}^{n} \omega_i R_i(r)$$

[1]

where ω_i ($0 \le \omega_i \le 1$ and such that, $\sum_{i=1}^{n} \omega_i = 1$) is a contributing weight of indicator "i". All the issue in the aggregation is how to assign the weights from available information (Clemen and Winkler, 1999; Liu et al., 2012; Winkler, 1968; Winkler and Cummings, 1972). In this work, we develop an approach that allows for the construction of weights such that the resulting aggregated distribution is a sort of weighted percentile in the ensemble of $R_i(r)$. To this end, we use the following two-parameter model for the weight (Eq. 2):

$$\omega_i = exp\left\{-\gamma\left(\frac{d_i}{\sigma}-b\right)^2\right\} \bigg/ \left[\sum_{j=1}^{n} exp\left\{-\gamma\left(\frac{d_j}{\sigma}-b\right)^2\right\}\right] \qquad [2]$$

where γ is the stiffness factor, b is the offset from a reference distribution, and d_i is the distance between the indicator "i" and the reference distribution.

More specifically, for the kind of problems we will be dealing with, the risk r_i for each indicator "i" has a functional form resulting from the product of three factors (Eq. 3),

$$r_i = \alpha z_i C \qquad [3]$$

where α is a scaling constant related to the exposure duration and the reference value of a pollutant (e.g., unit risk), C is the exposure concentration of the pollutant following a given route of exposure and z_i ($z_i > 0$) is a factor describing the characteristics of the exposure taken into account in indicator "i" to estimate the risk. In this case, risk r_i is random because z_i is often a random variable of distribution $f_i(z)$, and C is also distributed; all related by $R_i(r) = \int f_i(z)P(r/\alpha z)\,dz/[\alpha z]$, where $P(\cdots)$ is the distribution of C (see the list of abbreviations and terms in the footnote on the first page).

Eq. 3 is an approximation of the expression, $r_i = 1 - exp[-\alpha z_i C]$, in the limit of low concentrations of C. For the kind of risks described by Eq. 3, Eq. 1 is rewritten as follows: $R_c(r) = \sum_{i=1}^{n} \omega_i R_i(r) = \int dz \left[\frac{g(z)}{\alpha z}\right] \times P\left(\frac{r}{\alpha z}\right)$, where $g(z)$ is the consensus distribution resulting from the aggregation of the n indicator distributions, given by (Eq. 4):

$$g(z) = \sum_{i=1}^{n} \omega_i f_i(z) \qquad [4]$$

6

In this case, b in Eq. 2 is offset from reference distribution $g_r(z)$ (see below), d_i is the overlap distance between indicator "i" and the reference distribution calculated as (Eq. 5):

$$d_i = 1 - \text{overlap}[f_i, g_r] \qquad [5]$$

such that $0 \leq d_i \leq 1$, and σ is the standard deviation of the d_i's. See Fig. 1 for the general method to calculate the overlap (or overlapping area) between two functions.

Overlap between two functions

The overlap between $f_1(z)$ and $f_2(z)$ is the area under the intersecting curve between $f_1(z)$ and $f_2(z)$ as shown here:
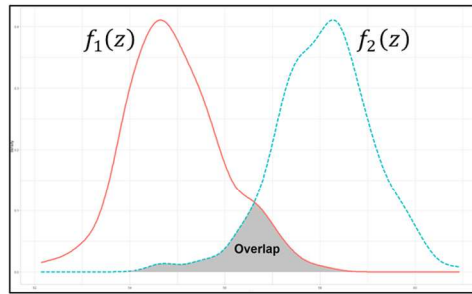
The overlap can be calculated as:

$$\text{overlap}[f_1, f_2] = \int \min_z[f_1(z), f_2(z)] \, dz$$

For numerical implementation, we consider that $f_1(z)$ and $f_2(z)$ are defined over the same set of $N + 1$ discrete points, $z_0, z_1, \cdots, z_N$, and we define the CDF of $f_i(z)$ as:

$$F_i(z) = \int^z f_i(z') \, dz' \longrightarrow F_{i,k} = \int^{z_k} f_i(z') \, dz'$$

As the area under the curve of $f_i(z)$ between z_{k-1} and z_k is given by, $\int_{z_{k-1}}^{z_k} f_i(z') \, dz' = F_{i,k} - F_{i,k-1}$, it follows that the overlap between $f_1(z)$ and $f_2(z)$ is obtained by:

$$\text{overlap}[f_1, f_2] = \sum_{k=1}^{N} \min\left[F_{1,k} - F_{1,k-1}, F_{2,k} - F_{2,k-1}\right]$$
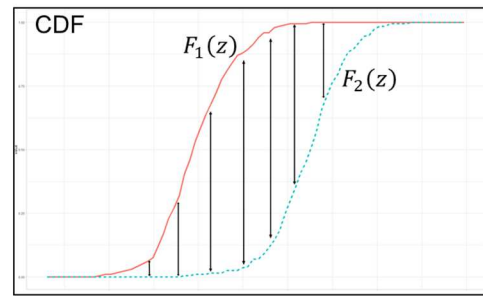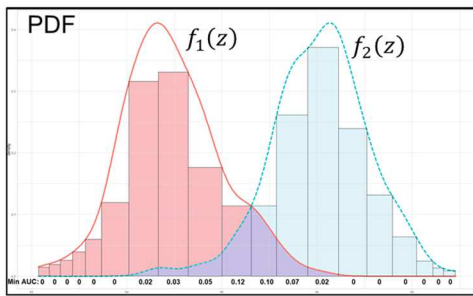
Fig. 1: General approach for calculating the overlap between two functions

Reference distribution $g_r(z)$ and two parameters b and γ in Eqs. 2 and 4 are determined as described in the following subsections.

2.1.1 Construction of $g_r(z)$

A reference distribution $g_r(z)$ can be constructed from $f_i(z)$ with (Eq. 6):

$$g_r(z) = \sum_{i=1}^{n} a_i f_i(z) \qquad [6]$$

where a_i ($0 \leq a_i \leq 1$ and such that $\sum_{i=1}^{n} a_i = 1$) are coefficients to be set. To determine the a_i coefficients and obtain an objective reference distribution, we require that $g_r(z)$ has a maximum overlap with all $f_i(z)$, i.e., to maximize total overlap A between $g_r(z)$ and all $f_i(z)$. The total overlap A is given as (Eq. 7):

$$A = \begin{pmatrix} 1 \\ 1 \\ \vdots \\ 1 \end{pmatrix}^T \underbrace{\begin{pmatrix} O_{11} & O_{12} & \cdots & O_{1n} \\ O_{21} & O_{22} & \cdots & O_{2n} \\ \vdots & \vdots & \vdots & \vdots \\ O_{n1} & O_{n2} & \cdots & O_{nn} \end{pmatrix}}_{\mathbf{O}} \begin{pmatrix} a_1 \\ a_2 \\ \vdots \\ a_n \end{pmatrix} \qquad [7]$$

where $O_{ij} = O_{ji} = \mathrm{overlap}[f_i, f_j]$ is the overlap between two (normalized to one) distribution functions $f_i(z)$ and $f_j(z)$, such that $O_{ii} = 1$. Overlap matrix $\mathbf{O}$ is symmetric with the trace, $\mathrm{Tr}(\mathbf{O}) = \sum_{k=1}^{n} \lambda_k = n$, where λ_k are the eigenvalues associated with (normalized to one) eigenvectors $\mathbf{v}_k$ of matrix $\mathbf{O}$ such that $0 \leq \lambda_1 < \lambda_2 < \cdots < \lambda_n \leq n$. For all coefficients a_i, the total overlap, $A = 1$ when there are zero overlaps $O_{ij} = 0$ for $i \neq j$, and $A = n$ when $O_{ij} = 1$. When $0 < O_{ij} < 1$, the maximum of the total overlap, A_{max}, is obtained by setting the a_i coefficients equal to eigenvector $\mathbf{v}_n$ corresponding to the largest eigenvalue λ_n (Eq. 8):

$$\begin{pmatrix} a_1 \\ a_2 \\ \vdots \\ a_n \end{pmatrix} = \frac{1}{\left[\sum_{i=1}^{n} v_{n,i}\right]} \begin{pmatrix} v_{n,1} \\ v_{n,2} \\ \vdots \\ v_{n,n} \end{pmatrix} \implies A_{max} = \lambda_n \frac{1}{\left[\sum_{i=1}^{n} v_{n,i}\right]} \begin{pmatrix} 1 \\ 1 \\ \vdots \\ 1 \end{pmatrix}^T \begin{pmatrix} v_{n,1} \\ v_{n,2} \\ \vdots \\ v_{n,n} \end{pmatrix} = \lambda_n \qquad [8]$$

This defines the weights of $g_r(z)$ in Eq. 6. Note, $v_{n,i} \geq 0$ should always be ensured. Additionally, note that $a_i = 1/n$ for all i in the case of zero overlaps, $O_{ij} = 0$ for $i \neq j$.

2.1.2 Determination of b

Now, let s denote a statistic (e.g., mean, median, 95th percentile…) of the consensus distribution $g(z)$, with the relation, $s = \sum_{i=1}^{n} \omega_i s_i$, where s_i is the same statistic associated to indicator "i". By construction, the shape of $s(b)$ as a function of b (via ω_i) is a logistic function of stiffness γ varying between s_r and $max(\{s_i\})$, where s_r is the statistic associated with reference distribution $g_r(z)$. Then, the parameter b in the weight can be chosen such that (Eq. 9):

$$s(b) = (1 - \theta)s_r + \theta \times max(\{s_i\}) \tag{9}$$

where θ (with $0 \leq \theta \leq 1$) is set a priori. $\theta = 0$ corresponds to the reference distribution for the consensus distribution, $g(z) = g_r(z)$, while $\theta = 1$ corresponds to $g(z) = f_i(z)$, for which $s_i = max(\{s_j\})$.

2.1.3 Determination of γ

The parameter γ can be set empirically depending on both the chosen offset parameter b and the selected logistic function form. To help in determining the relevant value of γ, it is possible to study logistic function $s(b)$ for different sets of parameters b and γ, as illustrated in the following sections.

2.2 Application of the CRI to inhalation cancer risk

To perform a cancer risk estimation, the most commonly encountered approach is to use an indicator that quantitatively estimates the exposure risk for a given route of exposure. Multiplying the concentration/dose of a specific chemical to a defined unit risk or slope factor is usually used to perform such estimation. Unit risks are estimates of the increased cancer risk from a specific route of exposure for lifetime exposure (US EPA, 2019). For instance, cancer inhalation unit risks (IURs) are estimates of the increased cancer risk for lifetime inhalation exposure to a concentration of 1 µg/m³ (US EPA, 2019). In contrast, inhalation cancer slope factors (CSFs) quantitatively describe the relationship between dose and response and are defined as $CSF\ (kg.day/mg) = IUR\ (m^3/mg) \times BW/IR = IUR\ (m^3/\mu g) \times 1,000 \times 70\ (kg)/20\ (m^3/day) = IUR\ (m^3/\mu g) \times 3,500$, where BW

represents the average body weight of an adult (70 kg) and *IR* represents the average inhalation rate of an adult (20 m^3/day) (Buonanno et al., 2015). Unit risks and CSFs are established by organizations and agencies for a given route of exposure and a given health effect based on animal and/or epidemiological studies. The simplest indicator is determined by multiplying the exposure concentrations by a unit risk, such as the IUR for inhalation exposure, while other indicators take into account different parameters of the exposure conditions (e.g., exposure duration) and/or the human characteristics (e.g., inhalation rate, body weight) to minimize the uncertainties in the risk estimation (Petit et al., 2019).

2.2.1 Cancer risk indicators for inhalation exposure

Eight cancer risk indicators for inhalation exposure were found in a previous work (Petit et al., 2019) (see Table 1). They all have a similar functional form and only differ in the expression of the z factor. For example, $z = 1$ for indicator RC and $z = (inhalation\ rate \times 3{,}500)/body\ weight$ for indicator ILCR3. The expressions of z for each indicator retrieved from the literature are highly variable and are given in Table 1.

Table 1: Expression of the z factor for each cancer risk indicator

Indicator	Expression of z	Reference
ILCR1	$z = \dfrac{\sqrt[3]{BW/70} \times IR_d \times 3{,}500}{BW \times PEF \times ET}$	Huang et al., 2016; Soltani et al., 2015
ILCR2	$z = \dfrac{\sqrt[3]{BW/70} \times IR_d \times cf \times 3{,}500}{BW \times ET}$	Chen and Liao, 2006; Hoseini et al., 2016; Singh et al., 2016; Wang et al., 2014
ILCR3	$z = \dfrac{IR_h \times 3{,}500}{BW}$	Hu et al., 2007; Li et al., 2013; Qu et al., 2015
ILCR4	$z = \dfrac{IR_h \times A \times 3{,}500}{BW \times ET}$	Li et al., 2014
ILCR5	$z = \dfrac{IR_d \times cf \times 3{,}500}{BW \times ET}$	Yu et al., 2015
LCR	$z = \dfrac{AT}{EF \times ET \times ED}$	Callen et al., 2014; Hsu et al., 2014; Jia et al., 2011; Lin et al., 2008; Liu et al., 2010; Ramirez et al., 2011; Wang et al., 2012
RC	$z = 1$	Irvine et al., 2014
RM	$z = \dfrac{IR_h \times BW \times cf}{BW \times IR_d}$	Amarillo et al., 2014

Note: A: inhalation absorption factor, AT: averaging time, BW: body weight, cf: conversion factor, ED: exposure duration, EF: exposure frequency, ET: exposure time, ILCR: incremental lifetime cancer risk, IR_d: inhalation rate per day, IR_h: inhalation rate per hour, LCR: lung cancer risk, PEF: particles emission factor, RC: cancer risk, RM: risk.

The cancer risk indicators were described and characterized by studying their z factor distribution. Table 2 provides the list of all input factors and their probability density functions (PDFs) that were used for the analysis of the z factor distribution for each risk indicator.

Table 2: List of input factors and their PDFs for the analysis of the z factor of each cancer risk indicator

Notation	Definition	Distribution/PDF	Parameters	Units	Indicator
ET	Exposure time	Constant	24	hour/day	RC, RM, $ILCR_3$
EF	Exposure frequency	Constant	365	day/year	RC, RM, $ILCR_{1,2,3,4,5}$
ED	Exposure duration	Constant	70	year	RC, RM, $ILCR_{1,2,3,4,5}$
AT	Averaging time	Constant	$365 \times 70 = 25{,}550$	day	RM, $ILCR_{1,2,3,4,5}$
AT	Averaging time	Constant	$24 \times 365 \times 70 = 613{,}200$	hour	RC
PEF	Particles emission factor	Constant	1.36×10^9	m^3/kg	$ILCR_1$
cf	Conversion factor	Constant	1×10^{-6} 1×10^3	mg/ng without dimension	$ILCR_{2,5}$ RM
IR_h	Inhalation rate	Log-normal	$\mu_{log} = 0.27$; $\sigma_{log} = 0.35$ [Allan et al., 2009]	$m^3/hour$	RM, $ILCR_{3,4}$
IR_d	Inhalation rate	Log-normal	$\mu_{log} = 2.76$; $\sigma_{log} = 0.23$ [Allan and Richardson, 1998]	m^3/day	RM, $ILCR_{1,2,5}$
BW	Body weight	Log-normal	$\mu_{log} = 4.09$; $\sigma_{log} = 0.30$ [Tanguy et al., 2007]	kg	RM, $ILCR_{1,2,3,4,5}$
A	Inhalation absorption factor	Beta*	$\alpha = 3 + \sqrt{2}$; $\beta = 6 - \alpha$	Unitless with $0 \leq A \leq 1$	$ILCR_4$

Note: Parameters of the inhalation rate PDF were derived from the reported studies. These studies provide the arithmetic mean (μ) and arithmetic standard deviation (σ). The natural logarithm mean (μ_{log}) and standard deviation (σ_{log}) values were calculated as follows:

$$\mu_{log} = \ln\left(\frac{\mu}{\sqrt{1+\frac{\sigma^2}{\mu^2}}}\right); \ \sigma_{log} = \sqrt{\ln\left(1 + \frac{\sigma^2}{\mu^2}\right)}.$$

* The associated mean and standard deviation of the chosen beta distribution are $\mu = 0.74$; $\sigma = 0.17$.

2.2.2. CRI and illustration of use

The CRI was generated following the approach outlined above in section 2.1. Statistic parameter s was set to the 90th percentile of z, while the parameter b was chosen to correspond to the equidistant point (50%) between s_r and $\max(s_i)$ with $\theta = 0.5$. To determine parameter γ, the logistic function was studied for different values of b and γ and was set in such a way that the stiffness was not too accentuated.

Once all parameters had been chosen, the z parameter of the CRI was determined. This z factor was unique for all the chemicals, route of exposure (here, inhalation), and exposure conditions considered. We chose to use the cancer IUR and/or inhalation CSF values from the Office of Environmental Health Hazard Assessment (OEHHA, 2019), US Environmental EPA Protection Agency (US EPA, 2018) and French Agency for Food, Environmental and Occupational Health & Safety (ANSES, 2019). The product $\alpha \times z$ in the CRI was determined for all chemicals with available cancer IUR and/or inhalation CSF values from the OEHHA, US EPA and ANSES for two exposure settings: environmental (lifetime inhalation exposure: 24 hours/day, 365 days/year for 70 years) (ATSDR, 2005; Cuadras et al., 2016; Korobitsyn, 2011; US EPA, 2005) and occupational (occupational inhalation exposure: 8 hours/day, 250 days/year for 45 years) (Park, 2018; Petit et al., 2019; Rhomberg et al., 2018). For a given chemical, if its cancer IUR was established by more than one of the three institutions had the same adverse outcome, we kept all available IURs. Any relevant or legitimate IUR can be used during a risk assessment.

Conducting a risk assessment is easy to implement because it only consists of multiplying "$\alpha \times z$", which are determined by the concentration distribution of a chemical. A user guide and an example demonstrating how to use CRI to conduct a risk assessment is illustrated: lifetime and occupational inhalation exposures to benzo[a]pyrene (BaP). For the sake of illustration, we used the BaP cancer IUR from the OEHHA and considered that the concentration distributions followed lognormal distributions (with the following parameters: $GM = 0.15 \, \mu g/m^3$ and $GSD = 4$ for BaP), while remaining constant over time. Following the convention used in France, we considered that for occupational exposure workers were exposed to a given substance for 8 hours a day, 5 days a week,

and 250 days a year for 45 years. Regarding lifetime exposures, we considered that people were exposed to a given substance for 24 hours a day, 7 days a week, 365 days a year for 70 years.

To aid the wider implementation of the consensus approach, a user friendly and interactive web application, named InCaRisk, has been created for cancer risk estimation using the CRI following inhalation exposure. This web application can also be used to compare existing cancer risk indicators with the CRI. It is built using the Shiny package in the R programming language (Chang et al., 2018), is free to access any device with an internet browser and requires no programming knowledge to use. It incorporates a variety of features to make it easy to use. This app is freely available to anyone who wants to use it.

2.3 Software

Data analyses and all calculations were performed with R software 4.0.2® (R Core Team, Vienna, Austria) for Windows 10©.

3. RESULTS

3.1 Cancer risk indicators: description and characterization

Among the eight cancer risk indicators given in Table 1, three (LCR, RC and RM) use the cancer IUR while five (all ILCR indicators) use the inhalation CSF, which is why the value '3,500' appears in the z expression of these five indicators (as a reminder $CSF\ (kg.day/mg) = IUR\ (m^3/\mu g) \times 3,500$). Differences between LCR, RC and RM arise when considering the exposure duration, time and frequency in RM and RC. RM differs from RC because it takes into account both the body weight and inhalation rate of an individual. Regarding the ILCR indicators, ILCR1 and ILCR2 differ from the other ILCRs because they account for the body weight variation of an individual compared to the average body weight found in the general population. ILCR1 is different from ILCR2 because it accounts for a particle emission factor from the emission source. ILCR3 differs from ILCR4 and ILCR5 because it accounts for the exposure time. Finally, ILCR4 is different from ILCR5 because it

takes into account an inhalation absorption factor. This factor ranges from 0 to 1, with 1 meaning that all of the inhaled pollutant is absorbed into the body.

Fig. 2 shows the PDF of each z factor from the eight cancer risk indicators generated using all input parameters given in Table 2. Anticipating the results for comparison purposes of each individual cancer risk indicator, the PDF of the z factor from the CRI is shown in Fig. 2 (see section 3.2 for the construction of the CRI). Two indicators (LCR and RC) are described by a delta distribution around $z = 1$, while all other indicators and the CRI followed a lognormal distribution, as confirmed by graphical views and statistical tests (Table 3).
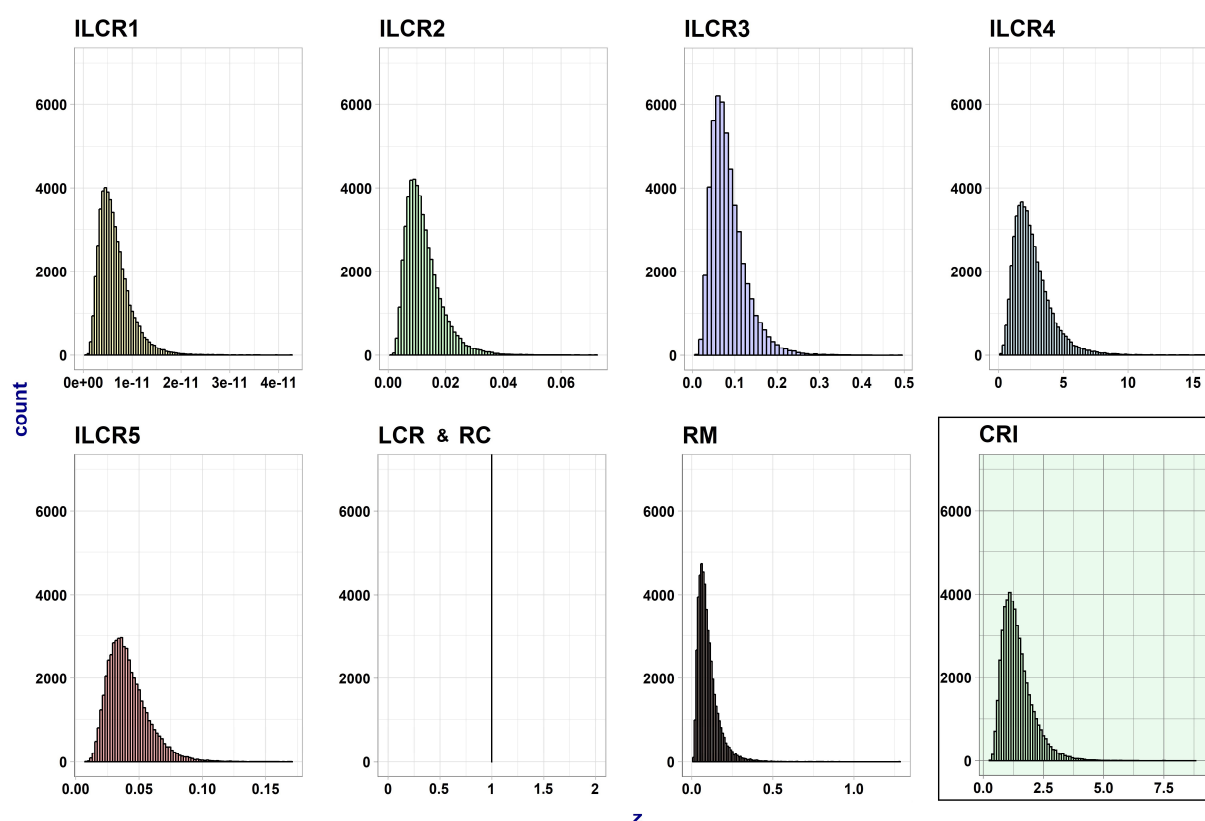
Fig. 2: Probability density function of the z parameter of each individual cancer risk indicator compared to that of the CRI

Table 3 provides the parameters of the distributions of the z factor for each individual cancer risk indicator and for the CRI, as well as the results from the normality and lognormality tests. The indicators ILCR2, ILCR3, ILCR5 and RM all have the natural logarithm mean values on the same order of magnitude. ILCR4 has the highest z values while ILCR1 has the lowest values by far.

Table 3: Characteristics of the *z* factor of each individual cancer risk indicator and the CRI

Indicator	μ	σ	Test of normality – p-value	Test of normality – conclusion	μ_{log}	σ_{log}	Test of lognormality – p-value	Test of lognormality – conclusion
ILCR1	6.5×10^{-12}	3.3×10^{-12}	$< 2.2 \times 10^{-16}$	Not normally distributed	-25.9	0.48	0.22	Lognormally distributed
ILCR2	0.01	0.006	$< 2.2 \times 10^{-16}$	Not normally distributed	-4.51	0.48	0.40	Lognormally distributed
ILCR3	0.09	0.04	3.0×10^{-15}	Not normally distributed	-2.57	0.47	0.55	Lognormally distributed
ILCR4	2.62	1.44	2.2×10^{-16}	Not normally distributed	0.83	0.53	0.61	Lognormally distributed
ILCR5	0.04	0.02	$< 2.2 \times 10^{-16}$	Not normally distributed	-3.26	0.38	0.23	Lognormally distributed
LCR	1.00	0.00	1	Normally distributed	0.00	0.00	1	Lognormally distributed
RC	1.00	0.00	1	Normally distributed	0.00	0.00	1	Lognormally distributed
RM	0.01	0.07	$< 2.2 \times 10^{-16}$	Not normally distributed	-2.48	0.59	0.78	Lognormally distributed
CRI	*1.44*	*0.66*	*$< 2.2 \times 10^{-16}$*	*Not normally distributed*	*0.27*	*0.42*	*0.10*	*Lognormally distributed*

Note: μ: the arithmetic mean, σ: arithmetic standard deviation, μ_{log}: natural logarithm mean value, σ_{log} natural logarithm standard deviation value, CRI: consensus cancer risk indicator.

Normality tests were performed using Shapiro-Wilk tests and QQ plots. Lognormality tests were performed using Shapiro-Wilk tests and QQ plots on the log transformed distributions.

3.2 CRI: construction, description and characterization

For the CRI construction, all the different parameters defined in Eqs. 1 to 9, have been determined and are presented in Table 4. It was found that the total overlap A_{max} between all z_i was equal to 2.2, denoting a low overlap (compared to the maximum theoretical overlap $A_{max} = 8$ for eight identical indicators) between each indicator, meaning that indicators lead to different values as seen, for instance, from the 90th percentile of the z distribution (parameter s_i in Table 4).

Table 4: Parameters obtained during the construction of the CRI

Indicator	a_i	s_i	d_i	ω_i
ILCR1	0.05	1.1×10^{-11}	0.01	0.06
ILCR2	0.10	0.02	0.01	0.06
ILCR3	0.30	0.14	0.01	0.06
ILCR4	0.002	4.44	0.50	0.46
ILCR5	0.23	0.06	0.006	0.06
LCR	3.1×10^{-5}	1	0.06	0.11
RC	3.1×10^{-5}	1	0.06	0.11
RM	0.30	0.18	0.02	0.07

Note: a_i: contribution weight of each indicator in the reference distribution (Eqs. 1, 2 and 4); ω_i: contribution weight of each indicator in the CRI (Eq. 1) such that the 90th percentile of z while the b parameter was chosen to correspond to the equidistant point ($\theta = 0.5$) between s_r and $\max(s_i)$ (e.g., when choosing $b = 2.19$ and $\gamma = 0.5$ in Fig. 3); d_i: empirical distance between the reference distribution and each indicator (Eq. 5); s_i: 90th percentile of the z distribution of each indicator (Eq. 9). σ the standard deviation of the d_i's (Eq. 2) was equal to 0.17.

Fig. 3 shows statistic $s(b)$ (the 90th percentile of the consensus z distribution) as a function of b and γ. As seen in the figure, the curve corresponded to a logistic curve ("S" shape or sigmoid curve), whose stiffness varied with γ. The chosen offset parameter b corresponded to the equidistant point (50%) between s_r (90th percentile of the z distribution of the reference distribution = 0.10) and $\max(s_i)$ (90th

percentile of the z distribution of ILCR4) and depended on the value of γ (Table 4 and Fig. 3). In what follows, we choose $b = 2.19$ and $\gamma = 0.5$.
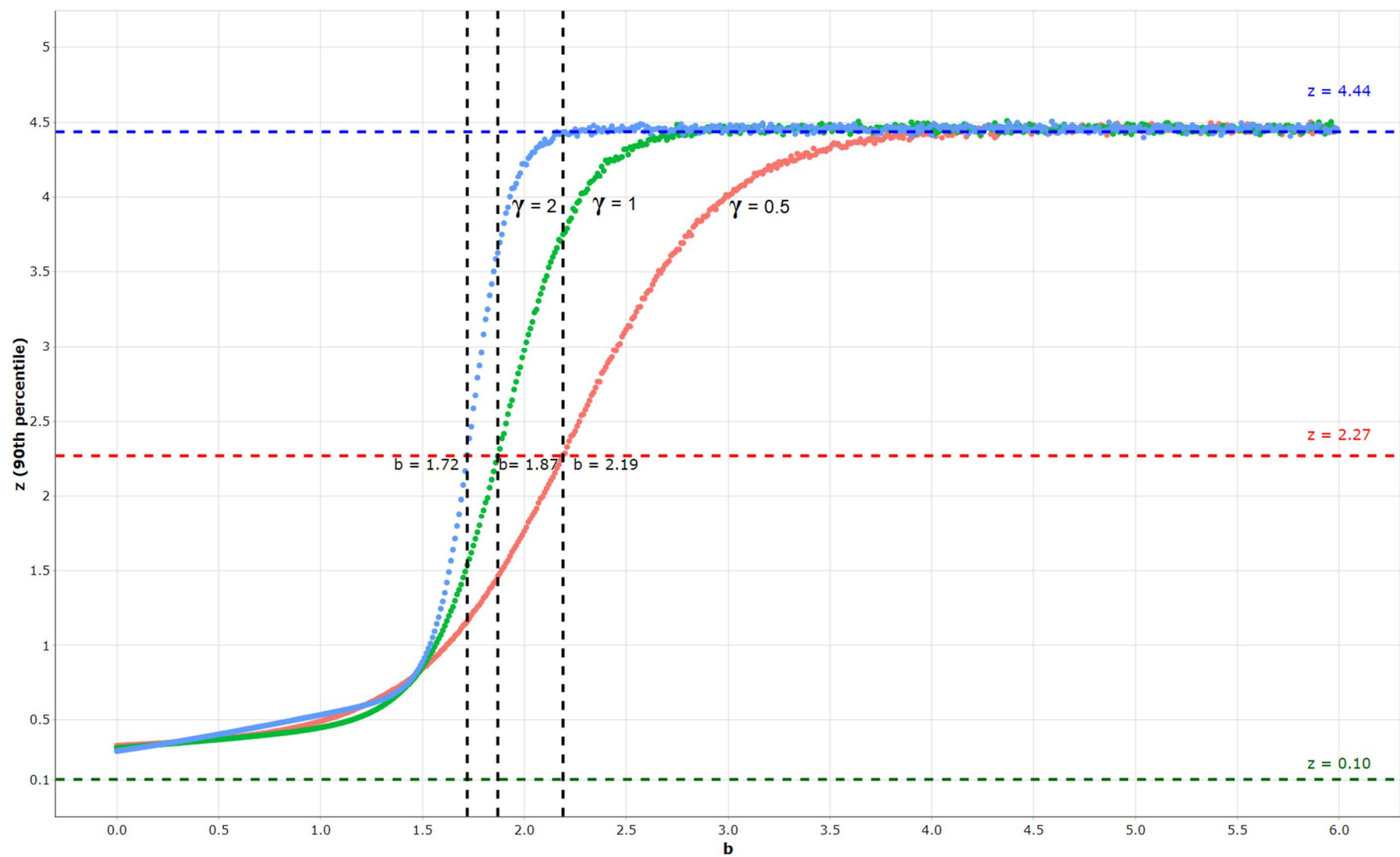
Fig. 3: Evolution of the 90th percentile of the consensus z distribution as a function of b and γ logistic curve

As constructed (Eqs. 1 to 9), the weights attributed to each cancer risk indicator in the CRI (ω_i) were the highest for risk indicators with the highest z (Table 4). The consensus z distribution, determined by the previously chosen parameters b and γ, appeared to be lognormally distributed, as seen graphically in Figs. 2 and 4. Fig. 4 shows the comparison between the PDF of the consensus z distribution and that of the theoretical empirical lognormal distribution (simulated) that would have been obtained by using the mean (μ_{log}) and standard deviation (σ_{log}) of the natural logarithm values from the consensus z distribution as input parameters. As seen graphically, both PDFs were the same. This was also confirmed through calculation: the empirical distance between the two PDFs was equal to 0.03, and the overlap was equal to 0.96. As a result, the consensus z distribution can be approximated (with an error of $1 - overlap = 1 - 0.96 = 0.04$ or 4%) to a lognormal distribution of parameters $\mu_{log} = 0.27$ (corresponding to a GM of 1.31) and $\sigma_{log} = 0.42$ (corresponding to a GSD of 1.53).
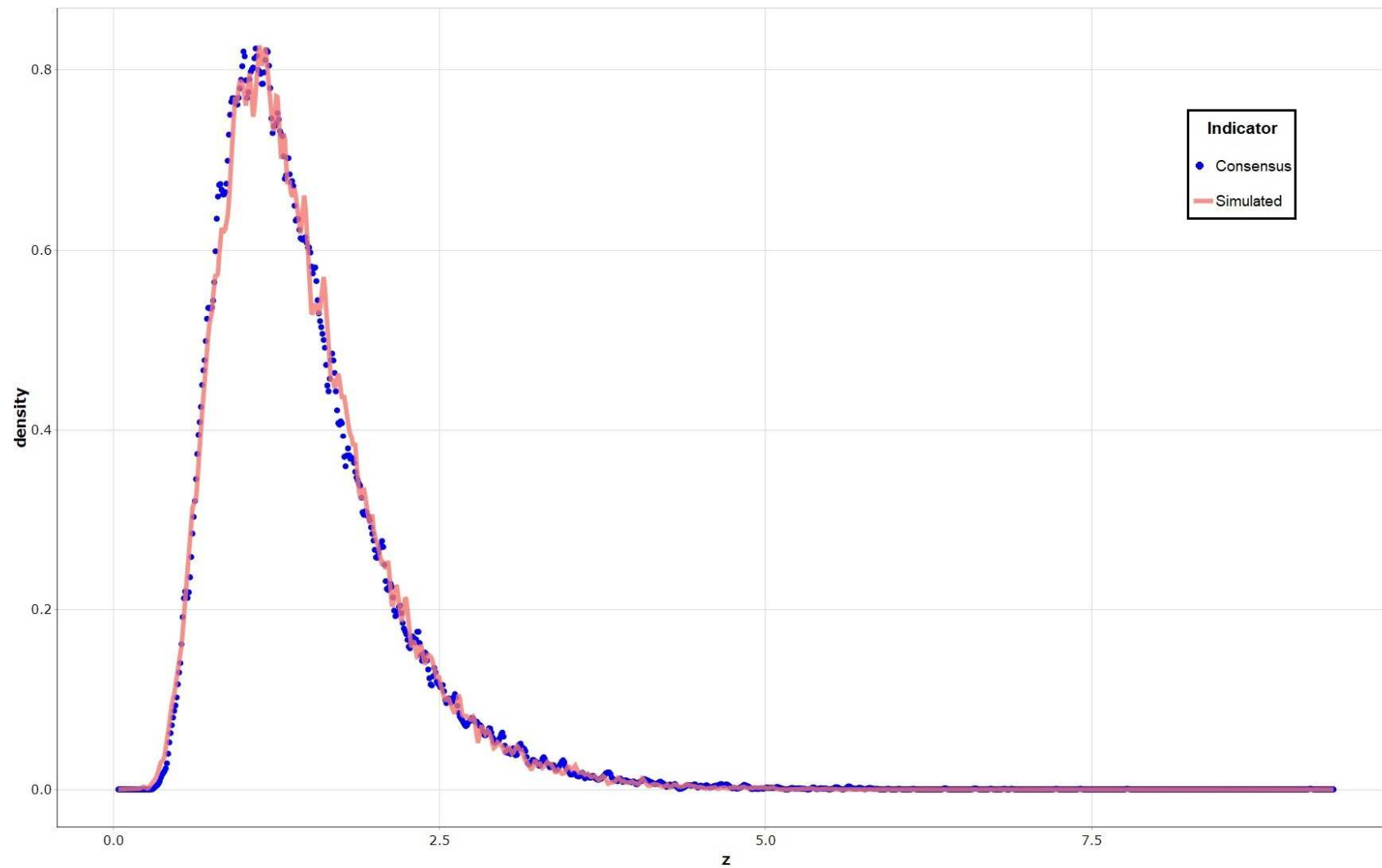
Fig. 4: Comparison of the PDF of the consensus z distribution and that of the theoretical empirical lognormal distribution (simulated) for 50,000 generated

values

3.3 Practical illustration of the use of the CRI

With the consensus z distribution, it is possible to assess risk by multiplying z by the concentration distribution (C) and coefficient α (Eq. 6).

3.3.1 Product $\alpha \times z$ for all chemicals with an IUR

Table 5 reports the main characteristics (tumor site, tumor type) regarding all cancer IUR values set by the OEHHA, US EPA and ANSES. Furthermore, the natural logarithm mean (μ_{log}) parameter of the lognormal distribution of the product $\alpha \times z$ was calculated for all 199 substances associated with cancer from inhalation exposures for two settings: environmental (lifetime exposure: 24 hours/day, 365 days/year for 70 years) and occupational (occupational exposure: 8 hours/day, 250 days/year for 45 years). The natural logarithm standard deviation (σ_{log}) is not reported in this table as it is by construction, always the same ($\sigma_{log} = 0.42$) regardless of the exposure setting and chemical considered.

Inhalation exposure does not necessarily lead to cancer of the respiratory tract. IURs were established for tumors in the digestive/gastrointestinal tract (46% of the time), neoplasms in the respiratory tract (35% of the time), tumors in the urinary tract (11% of the time), and endocrine, immune, neurologic, hematologic, hematopoietic, breast, reproductive, ocular or musculoskeletal cancers (8% of the time) (Table 5).

An interactive version of Table 5, which provides additional information regarding the cancer IUR establishment (incidence data source and extrapolation method/methodology), is available as supplemental material (Table A.1). Table A.1 goes beyond a simple inventory of cancer IUR and CSF values that can be found on the OEHHA, US EPA and ANSES websites. Table A.1 provides the cancer information with regard to these values and the incidence data source and extrapolation method used to establish them. To generate the interactive table, it is necessary to copy the text inside the box in the Supporting Material file, paste it into a text editor (e.g., Notepad) and save it as an .html file. Then, the supporting information can be viewed in any web browser. This interactive table provides

user friendly navigation, facilitates the understanding and manipulation of the data, and extracts information through possible queries. This interactive table is also available in the web application, under the "Data source" tab.

Table 5: Cancer information associated with the IUR and the product $\alpha \times z$ for all 199 substances associated with cancer from inhalation exposures

Substance	Chemical abstract number	IUR (m³/µg)	Source	IUR establishment: cancer information		Product $\alpha \times z$	
				Tumor site	Tumor type	Lifetime: μ_{log} (m³/µg)	Occupational: μ_{log} (m³/µg)
Acetaldehyde	75-07-0	2.70e-06	OEHHA, 2019	Respiratory	Nasal squamous cell carcinoma or adenocarcinoma	-12.5	-14.5
Acetaldehyde	75-07-0	2.20e-06	US EPA, 2018	Respiratory	Nasal squamous cell carcinoma or adenocarcinoma	-12.8	-14.7
Acetamide	60-35-5	2.00e-05	OEHHA, 2019	Digestive/Gastrointestinal	Liver tumor	-10.5	-12.5
Acetamide	60-35-5	2.00e-05	US EPA, 2018	Hematopoietic system	Hepatocellular carcinomas	-10.5	-12.5
Acrylamide	79-06-1	1.30e-03	OEHHA, 2019	Reproductive, Endocrine	Thyroid tumors and tunica vaginalis mesotheliomas	-6.37	-8.29
Acrylamide	79-06-1	1.00e-04	US EPA, 2018	Reproductive, Endocrine	Thyroid tumors and tunica vaginalis mesotheliomas	-8.94	-10.9
Acrylonitrile	107-13-1	2.90e-04	OEHHA, 2019	Respiratory	Respiratory tract cancer	-7.88	-9.79
Acrylonitrile	107-13-1	6.80e-05	US EPA, 2018	Respiratory	Respiratory cancer	-9.32	-11.2
Allyl chloride	107-05-1	6.00e-06	OEHHA, 2019	Digestive/Gastrointestinal	Forestomach tumor	-11.7	-13.7
Allyl chloride	107-05-1	6.00e-06	US EPA, 2018	Digestive/Gastrointestinal	Forestomach tumor	-11.7	-13.7
2-Aminoanthraquinone	117-79-3	9.40e-06	OEHHA, 2019	Digestive/Gastrointestinal	Liver tumor	-11.3	-13.2
2-Aminoanthraquinone	117-79-3	9.40e-06	US EPA, 2018	Digestive/Gastrointestinal	Liver tumor	-11.3	-13.2
Aniline	62-53-3	1.60e-06	OEHHA, 2019	Immune	Primary splenic sarcoma	-13.1	-15
Aniline	62-53-3	1.60e-06	US EPA, 2018	Immune	Primary splenic sarcoma	-13.1	-15
Arsenic	7440-38-2	3.30e-03	OEHHA, 2019	Respiratory	Lung tumor	-5.44	-7.36
Arsenic compounds	7440-38-2	4.30e-03	US EPA, 2018	Respiratory	Lung cancer	-5.18	-7.1
Asbestos	1332-21-4	1.90e-04	OEHHA, 2019	Respiratory	Lung tumor and mesothelioma	-8.29	-10.2
Benzene	71-43-2	2.90e-05	OEHHA, 2019	Hematologic	Leukemia	-10.2	-12.1
Benzene	71-43-2	2.60e-05	ANSES, 2019	Hematologic	Leukemia	-10.3	-12.2
Benzene	71-43-2	7.80e-06	US EPA, 2018	Hematologic	Leukemia	-11.5	-13.4
Benzidine	92-87-5	6.70e-02	US EPA, 2018	Urinary	Bladder tumors	-2.43	-4.35
Benzidine (and its salt)	92-87-5	1.40e-01	OEHHA, 2019	Urinary	Bladder tumor	-1.69	-3.61
Benzidine based dyes	1020	1.40e-01	OEHHA, 2019	Urinary	Bladder tumor	-1.69	-3.61
Direct Black 38	1937-37-7	1.40e-01	OEHHA, 2019	Urinary	Bladder tumor	-1.69	-3.61
Direct Blue 6	2602-46-2	1.40e-01	OEHHA, 2019	Urinary	Bladder tumor	-1.69	-3.61
Direct Brown 95 (technical grade)	16071-86-6	1.40e-01	OEHHA, 2019	Urinary	Bladder tumor	-1.69	-3.61
Benzyl chloride	100-44-7	4.90e-05	US EPA, 2018	Endocrine	C-cell thyroid tumor	-9.65	-11.6
Benzyl chloride	100-44-7	4.90e-05	OEHHA, 2019	Endocrine	C-cell thyroid tumor	-9.65	-11.6
Beryllium and compounds	7440-41-7 [1021]	2.40e-03	OEHHA, 2019	Respiratory	Lung tumor	-5.76	-7.68
Beryllium compounds	7440-41-7	2.40e-03	US EPA, 2018	Respiratory	Lung cancer	-5.76	-7.68
Dichloroethyl ether (Bis(2-chloroethyl)ether)	111-44-4	3.30e-04	US EPA, 2018	Hepatic	Hepatoma	-7.75	-9.67
Dichloroethyl ether (Bis(2-chloroethyl)ether)	111-44-4	7.10e-04	OEHHA, 2019	Digestive/Gastrointestinal	Hepatoma	-6.98	-8.89
Bis(chloromethyl)ether	542-88-1	6.20e-02	US EPA, 2018	Respiratory	Respiratory tract tumors	-2.51	-4.43
Bis(chloromethyl)ether	542-88-1	1.30e-02	OEHHA, 2019	Respiratory	Respiratory tract tumor	-4.07	-5.99
Potassium bromate	7758-01-2	1.40e-04	OEHHA, 2019	Urinary	Kidney tumor	-8.6	-10.5
1,3-Butadiene	106-99-0	3.00e-05	US EPA, 2018	Hematologic	Leukemia	-10.1	-12.1
1,3-Butadiene	106-99-0	1.70e-04	OEHHA, 2019	Respiratory	Lung alveolar and bronchiolar neoplasms	-8.41	-10.3
Cadmium compounds	7440-43-9	1.80e-03	US EPA, 2018	Respiratory	Lung, trachea, bronchus cancer	-6.05	-7.97
Cadmium and compounds	7440-43-9 [1045]	4.20e-03	OEHHA, 2019	Respiratory	Lung, trachea, bronchus cancer	-5.2	-7.12
Carbon tetrachloride (Tetrachloromethane)	56-23-5	6.00e-06	US EPA, 2018	Endocrine	Pheochromocytoma	-11.8	-13.7
Carbon tetrachloride (Tetrachloromethane)	56-23-5	4.20e-05	OEHHA, 2019	Digestive/Gastrointestinal	Liver tumor	-9.8	-11.7
Chlorinated paraffins	108171-26-2	2.50e-05	OEHHA, 2019	Digestive/Gastrointestinal	Liver tumor	-10.3	-12.2
4-Chloro-o-phenylenediamine	95-83-0	4.60e-06	OEHHA, 2019	Urinary	Urinary bladder tumor	-12	-13.9
Chloroform	67-66-3	5.30e-06	OEHHA, 2019	Urinary	Renal tumor	-11.9	-13.8

Continued Table 5

| Substance | Chemical abstract number | IUR (m³/µg) | Source | IUR establishment: cancer information | | Product $\alpha \times z$ | |
				Tumor site	Tumor type	Lifetime: μ_{log} (m³/µg)	Occupational: μ_{log} (m³/µg)
Chlorophenols	1060						
Pentachlorophenol	87-86-5	5.10e-06	US EPA, 2018	Digestive/Gastrointestinal	Liver tumor	-11.9	-13.8
Pentachlorophenol	87-86-5	5.10e-06	OEHHA, 2019	Digestive/Gastrointestinal	Liver tumor	-11.9	-13.8
2,4,6-Trichlorophenol	88-06-2	3.10e-06	US EPA, 2018	Hematologic	Leukemia	-12.4	-14.3
2,4,6-Trichlorophenol	88-06-2	2.00e-05	OEHHA, 2019	Digestive/Gastrointestinal	Reticulum cell sarcomas and heptomas	-10.5	-12.5
p-Chloro-o-toluidine	95-69-2	7.70e-05	OEHHA, 2019	Hematologic	Hemangioma and hemangiosarcoma tumor	-9.2	-11.1
Chromium (VI) compounds	18540-29-9	1.20e-02	US EPA, 2018	Respiratory	Lung cancer	-4.15	-6.07
Chromium 6+	18540-29-9	1.50e-01	OEHHA, 2019	Respiratory	Lung cancer	-1.62	-3.54
Barium chromate	10294-40-3	1.50e-01	OEHHA, 2019	Respiratory	Lung cancer	-1.62	-3.54
Calcium chromate	13765-19-0	1.50e-01	OEHHA, 2019	Respiratory	Lung cancer	-1.62	-3.54
Lead chromate	7758-97-6	1.50e-01	OEHHA, 2019	Respiratory	Lung cancer	-1.62	-3.54
Sodium dichromate	10588-01-9	1.50e-01	OEHHA, 2019	Respiratory	Lung cancer	-1.62	-3.54
Strontium chromate	7789-06-2	1.50e-01	OEHHA, 2019	Respiratory	Lung cancer	-1.62	-3.54
Chromium trioxide (as chromic acid mist)	1333-82-0	1.50e-01	OEHHA, 2019	Respiratory	Lung cancer	-1.62	-3.54
p-Cresidine	120-71-8	4.30e-05	OEHHA, 2019	Urinary	Urinary bladder tumor	-9.78	-11.7
Cupferron	135-20-6	6.30e-05	OEHHA, 2019	Hematologic	Hemangiosarcoma	-9.4	-11.3
2,4-Diaminoanisole	615-05-4	6.60e-06	OEHHA, 2019	Endocrine	Thyroid tumor	-11.7	-13.6
2,4-Toluene diamine	95-80-7	1.10e-03	US EPA, 2018	Breast	Mammary gland tumor	-6.54	-8.46
2,4-Toluene diamine	95-80-7	1.10e-03	OEHHA, 2019	Breast	Mammary gland tumor	-6.54	-8.46
1,2-Dibromo-3-chloropropane (DBCP)	96-12-8	2.00e-03	US EPA, 2018	Digestive/Gastrointestinal	Forestomach squamous cell carcinomas	-5.94	-7.86
1,2-Dibromo-3-chloropropane (DBCP)	96-12-8	2.00e-03	OEHHA, 2019	Digestive/Gastrointestinal	Forestomach squamous cell carcinomas	-5.94	-7.86
p-Dichlorobenzene	106-46-7	1.10e-05	US EPA, 2018	Digestive/Gastrointestinal	Hepatocarcinoma and adenoma	-11.1	-13.1
p-Dichlorobenzene	106-46-7	1.10e-05	OEHHA, 2019	Digestive/Gastrointestinal	Hepatocarcinoma and adenoma	-11.1	-13.1
3,3'-Dichlorobenzidine	91-94-1	3.40e-04	US EPA, 2018	Breast	Mammary adenocarcinoma	-7.71	-9.63
3,3'-Dichlorobenzidine	91-94-1	3.40e-04	OEHHA, 2019	Breast	Mammary adenocarcinoma	-7.71	-9.63
Ethylidene dichloride (1,1-Dichloroethane)	75-34-3	1.60e-06	US EPA, 2018	Breast	Mammary gland adenocarcinoma tumor	-13.1	-15
Ethylidene dichloride (1,1-Dichloroethane)	75-34-3	1.60e-06	OEHHA, 2019	Breast	Mammary gland adenocarcinoma tumor	-13.1	-15
Bis(2-ethylhexyl)phthalate (DEHP)	117-81-7	2.40e-06	US EPA, 2018	Digestive/Gastrointestinal	Hepatocellular carcinoma	-12.7	-14.6
Bis(2-ethylhexyl)phthalate (DEHP)	117-81-7	2.40e-06	OEHHA, 2019	Digestive/Gastrointestinal	Hepatocellular carcinoma	-12.7	-14.6
Diesel Exhaust	9901	3.00e-04	OEHHA, 2019	Respiratory	Lung tumor	-7.84	-9.76
Particulate emissions from diesel-fueled engines	9901	3.00e-04	OEHHA, 2019	Respiratory	Lung tumor	-7.84	-9.76
p-Dimethylaminoazobenzene	60-11-7	1.30e-03	US EPA, 2018	Digestive/Gastrointestinal	Liver tumor	-6.37	-8.29
p-Dimethylaminoazobenzene	60-11-7	1.30e-03	OEHHA, 2019	Digestive/Gastrointestinal	Liver tumor	-6.37	-8.29
2,4-Dinitrotoluene	121-14-2	8.90e-05	US EPA, 2018	Digestive/Gastrointestinal, Breast	Liver and mammary tumors	-9.05	-11
2,4-Dinitrotoluene	121-14-2	8.90e-05	OEHHA, 2019	Digestive/Gastrointestinal, Breast	Liver and mammary tumors	-9.05	-11
1,4-Dioxane (1,4-Diethylene dioxide)	123-91-1	5.00e-06	US EPA, 2018	Reproductive, Other, Hepatic, Urinary, Gastrointestinal, Respiratory	Multiple (nasal, liver, kidney, peritoneal, mammary gland, and Zymbal gland)	-11.9	-13.9
1,4-Dioxane (1,4-Diethylene dioxide)	123-91-1	7.70e-06	OEHHA, 2019	Digestive/Gastrointestinal, Breast	Hepatocellular carcinoma and adenoma	-11.5	-13.4
Epichlorohydrin (1-Chloro-2,3-epoxypropane)	106-89-8	1.20e-06	US EPA, 2018	Respiratory	Nasal cavity tumors	-13.4	-15.3
Epichlorohydrin (1-Chloro-2,3-epoxypropane)	106-89-8	2.30e-05	OEHHA, 2019	Digestive/Gastrointestinal, Breast	Forestomach papilloma and carcinoma	-10.4	-12.3

Continued Table 5

Substance	Chemical abstract number	IUR (m³/µg)	Source	Tumor site	Tumor type	Lifetime: μ_{log} (m³/µg)	Occupational: μ_{log} (m³/µg)
				IUR establishment: cancer information		Product $\alpha \times z$	
Ethyl benzene	100-41-4	2.50e-06	US EPA, 2018	Urinary	Renal tumor	-12.6	-14.5
Ethyl benzene	100-41-4	2.50e-06	OEHHA, 2019	Urinary	Renal tumor	-12.6	-14.5
1,2-Dibromoethane (ethylene dibromide)	106-93-4	6.00e-04	US EPA, 2018	Reproductive, Other, Respiratory	Nasal cavity (includes adenoma, adenocarcinoma, papillary adenoma, squamous cell carcinoma, and or/papilloma), hemangiosarcomas, mesotheliomas	-7.15	-9.07
1,2-Dibromoethane (ethylene dibromide)	106-93-4	7.10e-05	OEHHA, 2019	Respiratory	Nasal tumor	-9.28	-11.2
1,2-Dichloroethane (ethylene dichloride)	107-06-2	3.40e-06	ANSES, 2019	Breast	Mammary gland	-12.3	-14.2
1,2-Dichloroethane (ethylene dichloride)	107-06-2	2.60e-05	US EPA, 2018	Other	Hemangiosarcomas	-10.3	-12.2
1,2-Dichloroethane (ethylene dichloride)	107-06-2	2.10e-05	OEHHA, 2019	Hematologic	Hemangiosarcomas	-10.5	-12.4
Ethylene oxide (1,2-Epoxyethane)	75-21-8	3.00e-03	US EPA, 2018	Reproductive, Immune	Lymphoid cancer, (female) breast cancer	-5.54	-7.46
Ethylene oxide (1,2-Epoxyethane)	75-21-8	8.80e-05	OEHHA, 2019	Hematologic	Mononuclear cell leukemia	-9.06	-11
Ethylene thiourea	96-45-7	1.30e-05	US EPA, 2018	Endocrine	Thyroid tumor	-11	-12.9
Ethylene thiourea	96-45-7	1.30e-05	OEHHA, 2019	Endocrine	Thyroid tumor	-11	-12.9
Formaldehyde	50-00-0	1.30e-05	US EPA, 2018	Respiratory	Squamous cell carcinoma	-11	-12.9
Formaldehyde	50-00-0	6.00e-06	OEHHA, 2019	Respiratory	Nasal squamous cell carcinomas	-11.7	-13.7
Hexachlorobenzene	118-74-1	4.60e-04	US EPA, 2018	Hepatic	Hepatocellular carcinoma	-7.41	-9.33
Hexachlorobenzene	118-74-1	5.10e-04	OEHHA, 2019	Digestive/Gastrointestinal	Hepatoma and hepatocellular carcinoma	-7.31	-9.23
technical Hexachlorocyclohexane (HCH)	608-73-1	5.10e-04	US EPA, 2018	Hepatic	Liver nodules and hepatocellular carcinomas	-7.31	-9.23
Hexachlorocyclohexane (mixed or technical grade)	608-73-1	1.10e-03	OEHHA, 2019	Digestive/Gastrointestinal	Liver tumor	-6.54	-8.46
alpha-Hexachlorocyclohexane (a-HCH)	319-84-6	1.80e-03	US EPA, 2018	Hepatic	Hepatic nodules and hepatocellular carcinomas	-6.05	-7.97
alpha-Hexachlorocyclohexane (a-HCH)	319-84-6	1.10e-03	OEHHA, 2019	Digestive/Gastrointestinal	Hepatic nodules and hepatocellular carcinomas	-6.54	-8.46
beta-Hexachlorocyclohexane (b-HCH)	319-85-7	5.30e-04	US EPA, 2018	Hepatic	Hepatic nodules and hepatocellular carcinomas	-7.27	-9.19
beta-Hexachlorocyclohexane (b-HCH)	319-85-7	1.10e-03	OEHHA, 2019	Digestive/Gastrointestinal	Hepatic nodules and hepatocellular carcinomas	-6.54	-8.46
Lindane (gamma-Hexachlorocyclohexane)	58-89-9	3.10e-04	US EPA, 2018	Digestive/Gastrointestinal	Liver tumor	-7.8	-9.72
Lindane (gamma-Hexachlorocyclohexane)	58-89-9	3.10e-04	OEHHA, 2019	Digestive/Gastrointestinal	Liver tumor	-7.8	-9.72
Hydrazine	302-01-2	4.90e-03	US EPA, 2018	Respiratory	Nasal cavity adenoma or adenocarcinoma	-5.04	-6.96
Hydrazine	302-01-2	4.90e-03	OEHHA, 2019	Digestive/Gastrointestinal	Liver tumor	-5.04	-6.96
Lead and compounds	7439-92-1	1.20e-05	OEHHA, 2019	Urinary	Kidney tumor	-11.1	-13
Lead (inorganic)	1128	1.20e-05	OEHHA, 2019	Urinary	Kidney tumor	-11.1	-13
Lead acetate	301-04-2	1.20e-05	OEHHA, 2019	Urinary	Kidney tumor	-11.1	-13
Lead phosphate	7446-27-7	1.20e-05	OEHHA, 2019	Urinary	Kidney tumor	-11.1	-13
Lead subacetate	1335-32-6	1.20e-05	OEHHA, 2019	Urinary	Kidney tumor	-11.1	-13
Methyl tertiary-Butyl ether	1634-04-4	2.60e-07	US EPA, 2018	Urinary, Genital, Hematologic	Kidney adenomas and carcinomas, interstitial cell tumors, leukemia and lymphomas	-14.9	-16.8
Methyl tertiary-Butyl ether	1634-04-4	2.60e-07	OEHHA, 2019	Urinary, Genital, Hematologic	Kidney adenomas and carcinomas, interstitial cell tumors, leukemia and lymphomas	-14.9	-16.8
4,4'-Methylene bis(2-chloroaniline)	101-14-4	4.30e-04	US EPA, 2018	Urinary	Urinary bladder tumor	-7.48	-9.4
4,4'-Methylene bis(2-chloroaniline)	101-14-4	4.30e-04	OEHHA, 2019	Urinary	Urinary bladder tumor	-7.48	-9.4
Dichloromethane (Methylene chloride)	75-09-2	1.00e-08	US EPA, 2018	Hepatic, Respiratory	Hepatocellular carcinomas or adenomas, bronchoalveolar carcinomas or adenomas	-18.2	-20.1
Dichloromethane (Methylene chloride)	75-09-2	1.00e-06	OEHHA, 2019	Respiratory	Lung tumor	-13.5	-15.5
4,4'-Methylene dianiline	101-77-9	4.60e-04	US EPA, 2018	Digestive/Gastrointestinal	Liver tumor	-7.41	-9.33
4,4'-Methylene dianiline (and its dichloride)	101-77-9	4.60e-04	OEHHA, 2019	Digestive/Gastrointestinal	Liver tumor	-7.41	-9.33
Michler's ketone (4,4'-Bis(dimethylamino)benzophenone)	90-94-8	2.50e-04	OEHHA, 2019	Digestive/Gastrointestinal	Liver tumor	-8.02	-9.94

Continued Table 5

Substance	Chemical abstract number	IUR (m³/μg)	Source	Tumor site	Tumor type	Lifetime: μ_{log} (m³/μg)	Occupational: μ_{log} (m³/μg)
				IUR establishment: cancer information		Product $\alpha \times z$	
N-Nitrosidi-n-butylamine	924-16-3	3.10e-03	OEHHA, 2019	Urinary, Digestive/Gastrointestinal	Bladder and esophageal neoplasms	-5.5	-7.42
N-Nitrosodi-n-propylamine	621-64-7	2.00e-03	OEHHA, 2019	Digestive/Gastrointestinal	Liver tumor	-5.94	-7.86
N-Nitrosodiethylamine	55-18-5	1.00e-02	OEHHA, 2019	Digestive/Gastrointestinal	Hepatocellular neoplasms	-4.33	-6.25
N-Nitrosodimethylamine	62-75-9	1.40e-02	US EPA, 2018	Hepatic	Liver tumors	-4	-5.92
N-Nitrosodimethylamine	62-75-9	4.60e-03	OEHHA, 2019	Digestive/Gastrointestinal	Liver tumor	-5.11	-7.03
N-Nitrosodiphenylamine	86-30-6	2.60e-06	OEHHA, 2019	Urinary, Digestive/Gastrointestinal	Transitional-cell carcinomas of the bladder, hepatoma	-12.6	-14.5
N-Nitrosomorpholine	59-89-2	1.90e-03	US EPA, 2018	Respiratory	Respiratory tract tumor	-5.99	-7.91
N-Nitrosomorpholine	59-89-2	1.90e-03	OEHHA, 2019	Respiratory	Respiratory tract tumor	-5.99	-7.91
n-Nitroso-n-methylethylamine	10595-95-6	6.30e-03	OEHHA, 2019	Digestive/Gastrointestinal	Hepatocellular carcinoma	-4.79	-6.71
N-Nitrosopiperidine	100-75-4	2.70e-03	OEHHA, 2019	Digestive/Gastrointestinal	Liver tumor	-5.64	-7.56
N-Nitrosopyrrolidine	930-55-2	6.00e-04	OEHHA, 2019	Digestive/Gastrointestinal	Liver tumor	-7.14	-9.06
Nickel and compounds	7440-02-0	2.60e-04	OEHHA, 2019	Respiratory	Lung tumor	-7.98	-9.9
Nickel acetate	373-02-4	2.60e-04	OEHHA, 2019	Respiratory	Lung tumor	-7.98	-9.9
Nickel carbonate	3333-67-3	2.60e-04	OEHHA, 2019	Respiratory	Lung tumor	-7.98	-9.9
Nickel carbonyl	13463-39-3	2.60e-04	OEHHA, 2019	Respiratory	Lung tumor	-7.98	-9.9
Nickel hydroxide	12054-48-7	2.60e-04	OEHHA, 2019	Respiratory	Lung tumor	-7.98	-9.9
Nickel oxide	1313-99-1	2.60e-04	OEHHA, 2019	Respiratory	Lung tumor	-7.98	-9.9
Nickel refinery dust from the pyrometallurgical process	1146	2.60e-04	OEHHA, 2019	Respiratory	Lung tumor	-7.98	-9.9
Nickel refinery dust	1146	2.40e-04	US EPA, 2018	Respiratory	Lung cancer	-8.07	-9.98
Nickel subsulfide	12035-72-2	2.60e-04	OEHHA, 2019	Respiratory	Lung tumor	-7.98	-9.9
Nickel subsulfide	12035-72-2	4.80e-04	US EPA, 2018	Respiratory	Lung cancer	-7.37	-9.29
Nickelocene	1271-28-9	2.60e-04	OEHHA, 2019	Respiratory	Lung tumor	-7.98	-9.9
p-Nitrosodiphenylamine	156-10-5	6.30e-06	OEHHA, 2019	Digestive/Gastrointestinal	Liver tumor	-11.7	-13.6
Perchloroethylene (Tetrachloroethylene)	127-18-4	2.60e-07	ANSES, 2019	Hepatic	Hepatocellular adenomas and carcinomas	-14.9	-16.8
Perchloroethylene (Tetrachloroethylene)	127-18-4	2.60e-07	US EPA, 2018	Hepatic	Hepatocellular adenomas or carcinomas	-14.9	-16.8
Perchloroethylene (Tetrachloroethylene)	127-18-4	6.10e-06	OEHHA, 2019	Digestive/Gastrointestinal	Hepatocellular adenoma and carcinoma	-11.7	-13.7
PCB (Polychlorinated biphenyls)	1336-36-3	1.00e-04	US EPA, 2018	Hepatic	Liver hepatocellular adenomas, carcinomas, cholangiomas, or cholangiocarcinomas	-8.94	-10.9
PCB (Polychlorinated biphenyls) (unspeciated mixture) (lowest risk)	1336-36-3	2.00e-05	OEHHA, 2019	Digestive/Gastrointestinal	Liver tumor	-10.5	-12.5
PCB (Polychlorinated biphenyls) (unspeciated mixture) (low risk)	1336-36-3	1.10e-04	OEHHA, 2019	Digestive/Gastrointestinal	Liver tumor	-8.84	-10.8
PCB (Polychlorinated biphenyls) (unspeciated mixture) (high risk)	1336-36-3	5.70e-04	OEHHA, 2019	Digestive/Gastrointestinal	Liver tumor	-7.2	-9.11
PCB (Polychlorinated biphenyls) (speciated)							
3,3',4,4'-Tetrachlorobiphenyl (PCB 77)	32598-13-3	3.80e-03	OEHHA, 2019	Digestive/Gastrointestinal	Liver tumor	-5.3	-7.22
3,4,4',5-Tetrachlorobiphenyl (PCB 81)	70362-50-4	1.10e-02	OEHHA, 2019	Digestive/Gastrointestinal	Liver tumor	-4.24	-6.15
2,3,3',4,4'-Pentachlorobiphenyl (PCB 105)	32598-14-4	1.10e-03	OEHHA, 2019	Digestive/Gastrointestinal	Liver tumor	-6.54	-8.46
2,3,4,4',5-Pentachlorobiphenyl (PCB 114)	74472-37-0	1.10e-03	OEHHA, 2019	Digestive/Gastrointestinal	Liver tumor	-6.54	-8.46
2,3',4,4',5-Pentachlorobiphenyl (PCB 118)	31508-00-6	1.10e-03	OEHHA, 2019	Digestive/Gastrointestinal	Liver tumor	-6.54	-8.46
2,3',4,4',5'-Pentachlorobiphenyl (PCB 123)	65510-44-3	1.10e-03	OEHHA, 2019	Digestive/Gastrointestinal	Liver tumor	-6.54	-8.46
3,3',4,4',5-Pentachlorobiphenyl (PCB 126)	57465-28-8	3.80e+00	OEHHA, 2019	Digestive/Gastrointestinal	Liver tumor	1.61	-0.31
2,3,3',4,4',5-Hexachlorobiphenyl (PCB 156)	38380-08-4	1.10e-03	OEHHA, 2019	Digestive/Gastrointestinal	Liver tumor	-6.54	-8.46
2,3,3',4,4',5'-Hexachlorobiphenyl (PCB 157)	69782-90-7	1.10e-03	OEHHA, 2019	Digestive/Gastrointestinal	Liver tumor	-6.54	-8.46
2,3',4,4',5,5'-Hexachlorobiphenyl (PCB 167)	52663-72-6	1.10e-03	OEHHA, 2019	Digestive/Gastrointestinal	Liver tumor	-6.54	-8.46
3,3',4,4',5,5'-Hexachlorobiphenyl (PCB 169)	32774-16-6	1.10e+00	OEHHA, 2019	Digestive/Gastrointestinal	Liver tumor	0.37	-1.55
2,3,3',4,4',5,5'-Heptachlorobiphenyl (PCB 189)	39635-31-9	1.10e-03	OEHHA, 2019	Digestive/Gastrointestinal	Liver tumor	-6.54	-8.46

Continued Table 5

| Substance | Chemical abstract number | IUR (m³/µg) | Source | IUR establishment: cancer information | | Product $\alpha \times z$ | |
				Tumor site	Tumor type	Lifetime: μ_{log} (m³/µg)	Occupational: μ_{log} (m³/µg)
Polychlorinated Dibenzo-p-Dioxins (PCDD) (Treated as 2,3,7,8-TCDD for HRA)	1085	3.80e+01	OEHHA, 2019	Digestive/Gastrointestinal	Liver neoplastic nodule or hepatocellular carcinoma	3.91	1.99
1,2,3,4,6,7,8,9-Octachlorodibenzo-p-dioxin	3268-87-9	1.10e-02	OEHHA, 2019	Digestive/Gastrointestinal	Liver neoplastic nodule or hepatocellular carcinoma	-4.24	-6.15
1,2,3,4,6,7,8-Heptachlorodibenzo-p-dioxin	35822-46-9	3.80e-01	OEHHA, 2019	Digestive/Gastrointestinal	Liver neoplastic nodule or hepatocellular carcinoma	-0.69	-2.61
1,2,3,4,7,8-Hexachlorodibenzo-p-dioxin	39227-28-6	3.80e+00	OEHHA, 2019	Digestive/Gastrointestinal	Liver neoplastic nodule or hepatocellular carcinoma	1.61	-0.31
1,2,3,6,7,8-Hexachlorodibenzo-p-dioxin	57653-85-7	3.80e+00	OEHHA, 2019	Digestive/Gastrointestinal	Liver neoplastic nodule or hepatocellular carcinoma	1.61	-0.31
1,2,3,7,8,9-Hexachlorodibenzo-p-dioxin	19408-74-3	3.80e+00	OEHHA, 2019	Digestive/Gastrointestinal	Liver neoplastic nodule or hepatocellular carcinoma	1.61	-0.31
1,2,3,7,8-Pentachlorodibenzo-p-dioxin	40321-76-4	3.80e+01	OEHHA, 2019	Digestive/Gastrointestinal	Liver neoplastic nodule or hepatocellular carcinoma	3.91	1.99
2,3,7,8-Tetrachlorodibenzo-p-dioxin	1746-01-6	3.80e+01	US EPA, 2018	Digestive/Gastrointestinal	Liver neoplastic nodule or hepatocellular carcinoma	3.91	1.99
2,3,7,8-Tetrachlorodibenzo-p-dioxin	1746-01-6	3.80e+01	OEHHA, 2019	Digestive/Gastrointestinal	Liver neoplastic nodule or hepatocellular carcinoma	3.91	1.99
Hexachlorodibenzo-p-dioxin, mixture	19408-74-3	1.30e+00	US EPA, 2018	Digestive/Gastrointestinal	Liver neoplastic nodule or hepatocellular carcinoma	0.532	-1.39
Polychlorinated Dibenzofurans (PCDF) (Treated as 2,3,7,8-TCDD for HRA)	1080	3.80e+01	OEHHA, 2019	Digestive/Gastrointestinal	Liver neoplastic nodule or hepatocellular carcinoma	3.91	1.99
1,2,3,4,6,7,8,9-Octachlorodibenzofuran	39001-02-0	1.10e-02	OEHHA, 2019	Digestive/Gastrointestinal	Liver neoplastic nodule or hepatocellular carcinoma	-4.24	-6.15
1,2,3,4,6,7,8-Heptachlorodibenzofuran	67562-39-4	3.80e-01	OEHHA, 2019	Digestive/Gastrointestinal	Liver neoplastic nodule or hepatocellular carcinoma	-0.69	-2.61
1,2,3,4,7,8,9-Heptachlorodibenzofuran	55673-89-7	3.80e-01	OEHHA, 2019	Digestive/Gastrointestinal	Liver neoplastic nodule or hepatocellular carcinoma	-0.69	-2.61
1,2,3,4,7,8-Hexachlorodibenzofuran	70648-26-9	3.80e+00	OEHHA, 2019	Digestive/Gastrointestinal	Liver neoplastic nodule or hepatocellular carcinoma	1.61	-0.31
1,2,3,6,7,8-Hexachlorodibenzofuran	57117-44-9	3.80e+00	OEHHA, 2019	Digestive/Gastrointestinal	Liver neoplastic nodule or hepatocellular carcinoma	1.61	-0.31
1,2,3,7,8,9-Hexachlorodibenzofuran	72918-21-9	3.80e+00	OEHHA, 2019	Digestive/Gastrointestinal	Liver neoplastic nodule or hepatocellular carcinoma	1.61	-0.31
1,2,3,7,8-Pentachlorodibenzofuran	57117-41-6	1.10e+00	OEHHA, 2019	Digestive/Gastrointestinal	Liver neoplastic nodule or hepatocellular carcinoma	0.37	-1.55
2,3,4,6,7,8-Hexachlorodibenzofuran	60851-34-5	3.80e+00	OEHHA, 2019	Digestive/Gastrointestinal	Liver neoplastic nodule or hepatocellular carcinoma	1.61	-0.31
2,3,4,7,8-Pentachlorodibenzofuran	57117-31-4	1.10e+01	OEHHA, 2019	Digestive/Gastrointestinal	Liver neoplastic nodule or hepatocellular carcinoma	2.67	0.75
2,3,7,8-Tetrachlorodibenzofuran	5120-73-19	3.80e+00	OEHHA, 2019	Digestive/Gastrointestinal	Liver neoplastic nodule or hepatocellular carcinoma	1.61	-0.31
Polycyclic Aromatic Hydrocarbon (PAH) [Treated as B(a)P for HRA]	1150	1.10e-03	OEHHA, 2019	Respiratory	Respiratory tract tumor	-6.54	-8.46
1,6-Dinitropyrene	42397-64-8	6.00e-03	US EPA, 2018	Respiratory	Respiratory tract tumor	-4.85	-6.77
1,6-Dinitropyrene	42397-64-8	1.10e-02	OEHHA, 2019	Respiratory	Respiratory tract tumor	-4.24	-6.15
1,8-Dinitropyrene	42397-65-9	6.00e-04	US EPA, 2018	Respiratory	Respiratory tract tumor	-7.15	-9.07
1,8-Dinitropyrene	42397-65-9	1.10e-03	OEHHA, 2019	Respiratory	Respiratory tract tumor	-6.54	-8.46
1-Nitropyrene	5522-43-0	6.00e-05	US EPA, 2018	Respiratory	Respiratory tract tumor	-9.45	-11.4
1-Nitropyrene	5522-43-0	1.10e-04	OEHHA, 2019	Respiratory	Respiratory tract tumor	-8.84	-10.8
2-Nitrofluorene	607-57-8	6.00e-06	US EPA, 2018	Respiratory	Respiratory tract tumor	-11.8	-13.7
2-Nitrofluorene	607-57-8	1.10e-05	OEHHA, 2019	Respiratory	Respiratory tract tumor	-11.1	-13.1
3-Methylcholanthrene	56-49-5	6.30e-03	US EPA, 2018	Respiratory	Respiratory tract tumor	-4.8	-6.72
3-Methylcholanthrene	56-49-5	6.30e-03	OEHHA, 2019	Respiratory	Respiratory tract tumor	-4.79	-6.71
4-Nitropyrene	57835-92-4	6.00e-05	US EPA, 2018	Respiratory	Respiratory tract tumor	-9.45	-11.4
4-Nitropyrene	57835-92-4	1.10e-04	OEHHA, 2019	Respiratory	Respiratory tract tumor	-8.84	-10.8
5-Methylchrysene	3697-24-3	6.00e-04	US EPA, 2018	Respiratory	Respiratory tract tumor	-7.15	-9.07
5-Methylchrysene	3697-24-3	1.10e-03	OEHHA, 2019	Respiratory	Respiratory tract tumor	-6.54	-8.46
5-Nitroacenaphthene	602-87-9	3.70e-05	US EPA, 2018	Respiratory	Respiratory tract tumor	-9.93	-11.9
5-Nitroacenaphthene	602-87-9	3.70e-05	OEHHA, 2019	Respiratory	Respiratory tract tumor	-9.93	-11.8
6-Nitrochrysene	7496-02-8	1.10e-02	OEHHA, 2019	Respiratory	Respiratory tract tumor	-4.24	-6.15
6-Nitrochrysene	7496-02-8	6.00e-03	US EPA, 2018	Respiratory	Respiratory tract tumor	-4.85	-6.77
7,12-Dimethylbenz[a]anthracene	57-97-6	7.10e-02	US EPA, 2018	Respiratory	Respiratory tract tumor	-2.38	-4.29
7,12-Dimethylbenz[a]anthracene	57-97-6	7.10e-02	OEHHA, 2019	Respiratory	Respiratory tract tumor	-2.37	-4.29
7H-Dibenzo[c,g]carbazole	194-59-2	6.00e-04	US EPA, 2018	Respiratory	Respiratory tract tumor	-7.15	-9.07
7H-Dibenzo[c,g]carbazole	194-59-2	1.10e-03	OEHHA, 2019	Respiratory	Respiratory tract tumor	-6.54	-8.46

Continued Table 5

Substance	Chemical abstract number	IUR (m³/µg)	Source	Tumor site	Tumor type	Product $\alpha \times z$ Lifetime: μ_{log} (m³/µg)	Occupational: μ_{log} (m³/µg)
				IUR establishment: cancer information			
Benz[a]anthracene	56-55-3	6.00e-05	US EPA, 2018	Respiratory	Respiratory tract tumor	-9.45	-11.4
Benz[a]anthracene	56-55-3	1.10e-04	OEHHA, 2019	Respiratory	Respiratory tract tumor	-8.84	-10.8
Benzo[a]pyrene	50-32-8	1.10e-03	OEHHA, 2019	Respiratory	Respiratory tract tumor	-6.54	-8.46
Benzo[a]pyrene	50-32-8	6.00e-04	US EPA, 2018	Gastrointestinal, Respiratory	Squamous cell neoplasia in the larynx, pharynx, trachea, nasal cavity, esophagus, and forestomach	-7.15	-9.07
Benzo[a]pyrene toxic equivalent (BaPeq)	50-32-8	1.10e-03	OEHHA, 2019	Respiratory	Respiratory tract tumor	-6.54	-8.46
Benzo[b]fluoranthene	205-99-2	6.00e-05	US EPA, 2018	Respiratory	Respiratory tract tumor	-9.45	-11.4
Benzo[b]fluoranthene	205-99-2	1.10e-04	OEHHA, 2019	Respiratory	Respiratory tract tumor	-8.84	-10.8
Benzo[j]fluoranthene	205-82-3	6.00e-05	US EPA, 2018	Respiratory	Respiratory tract tumor	-9.45	-11.4
Benzo[j]fluoranthene	205-82-3	1.10e-04	OEHHA, 2019	Respiratory	Respiratory tract tumor	-8.84	-10.8
Benzo[k]fluoranthene	207-08-9	6.00e-06	US EPA, 2018	Respiratory	Respiratory tract tumor	-11.8	-13.7
Benzo[k]fluoranthene	207-08-9	1.10e-04	OEHHA, 2019	Respiratory	Respiratory tract tumor	-8.84	-10.8
Chrysene	218-01-9	6.00e-07	US EPA, 2018	Respiratory	Respiratory tract tumor	-14.1	-16
Chrysene	218-01-9	1.10e-05	OEHHA, 2019	Respiratory	Respiratory tract tumor	-11.1	-13.1
Dibenz[a,h]acridine	226-36-8	6.00e-05	US EPA, 2018	Respiratory	Respiratory tract tumor	-9.45	-11.4
Dibenz[a,h]acridine	226-36-8	1.10e-04	OEHHA, 2019	Respiratory	Respiratory tract tumor	-8.84	-10.8
Dibenz[a,h]anthracene	53-70-3	6.00e-04	US EPA, 2018	Respiratory	Respiratory tract tumor	-7.15	-9.07
Dibenz[a,h]anthracene	53-70-3	1.20e-03	OEHHA, 2019	Respiratory	Respiratory tract tumor	-6.45	-8.37
Dibenz[a,j]acridine	224-42-0	6.00e-05	US EPA, 2018	Respiratory	Respiratory tract tumor	-9.45	-11.4
Dibenz[a,j]acridine	224-42-0	1.10e-04	OEHHA, 2019	Respiratory	Respiratory tract tumor	-8.84	-10.8
Dibenzo[a,e]pyrene	192-65-4	6.00e-04	US EPA, 2018	Respiratory	Respiratory tract tumor	-7.15	-9.07
Dibenzo[a,e]pyrene	192-65-4	1.10e-03	OEHHA, 2019	Respiratory	Respiratory tract tumor	-6.54	-8.46
Dibenzo[a,h]pyrene	189-64-0	6.00e-03	US EPA, 2018	Respiratory	Respiratory tract tumor	-4.85	-6.77
Dibenzo[a,h]pyrene	189-64-0	1.10e-02	OEHHA, 2019	Respiratory	Respiratory tract tumor	-4.24	-6.15
Dibenzo[a,i]pyrene	189-55-9	6.00e-03	US EPA, 2018	Respiratory	Respiratory tract tumor	-4.85	-6.77
Dibenzo[a,i]pyrene	189-55-9	1.10e-02	OEHHA, 2019	Respiratory	Respiratory tract tumor	-4.24	-6.15
Dibenzo[a,l]pyrene	191-30-0	6.00e-03	US EPA, 2018	Respiratory	Respiratory tract tumor	-4.85	-6.77
Dibenzo[a,l]pyrene	191-30-0	1.10e-02	OEHHA, 2019	Respiratory	Respiratory tract tumor	-4.24	-6.15
Indeno[1,2,3-cd]pyrene	193-39-5	6.00e-05	US EPA, 2018	Respiratory	Respiratory tract tumor	-9.45	-11.4
Indeno[1,2,3-cd]pyrene	193-39-5	1.10e-04	OEHHA, 2019	Respiratory	Respiratory tract tumor	-8.84	-10.8
Naphthalene	91-20-3	5.60e-06	ANSES, 2019	Respiratory	Nasal olfactory epithelial neuroblastoma	-11.9	-13.9
Naphthalene	91-20-3	3.40e-05	US EPA, 2018	Respiratory	Nasal respiratory epithelial adenoma and nasal olfactory epithelial neuroblastoma	-10	-11.9
Naphthalene	91-20-3	3.40e-05	OEHHA, 2019	Respiratory	Nasal respiratory epithelial adenoma and nasal olfactory epithelial neuroblastoma	-10	-11.9
Coke Oven Emissions	8007-45-2	6.20e-04	US EPA, 2018	Respiratory	Respiratory cancer	-7.12	-9.03
1,3-Propane sultone	1120-71-4	6.90e-04	US EPA, 2018	Neurologic	Cerebellar malignant glioma tumor	-7	-8.92
1,3-Propane sultone	1120-71-4	6.90e-04	OEHHA, 2019	Neurologic	Cerebellar malignant glioma tumor	-7	-8.92
Propylene oxide	75-56-9	3.70e-06	US EPA, 2018	Respiratory	Nasal cavity hemangioma or hemangiosarcoma	-12.2	-14.2
Propylene oxide	75-56-9	3.70e-06	OEHHA, 2019	Digestive/Gastrointestinal	Forestomach squamous cell carcinoma tumor	-12.2	-14.2
1,1,2,2-Tetrachloroethane	79-34-5	5.80e-05	OEHHA, 2019	Digestive/Gastrointestinal	Hepatocellular carcinoma tumor	-9.48	-11.4
Tetrachlorophenols (see Chlorophenols)							
2,4,5-Trichlorophenol (see Chlorophenols)							
2,4,6-Trichlorophenol (see Chlorophenols)							

Continued Table 5

Substance	Chemical abstract number	IUR (m³/µg)	Source	Tumor site	Tumor type	Lifetime: μ_{log} (m³/µg)	Occupational: μ_{log} (m³/µg)
				IUR establishment: cancer information		**Product $\alpha \times z$**	
Thioacetamide	62-55-5	1.70e-03	OEHHA, 2019	Digestive/Gastrointestinal	Liver tumor	-6.1	-8.02
Toluene diisocyantates	26471-62-5	1.10e-05	OEHHA, 2019	Musculoskeletal	Subcutaneous fibroma/fibrosarcoma tumor	-11.1	-13.1
Toluene-2,4-diisocyantates	584-84-9	1.10e-05	OEHHA, 2019	Musculoskeletal	Subcutaneous fibroma/fibrosarcoma tumor	-11.1	-13.1
Toluene-2,6-diisocyanate	91-08-7	1.10e-05	OEHHA, 2019	Musculoskeletal	Subcutaneous fibroma/fibrosarcoma tumor	-11.1	-13.1
1,1,2-Trichloroethane (Vinyl trichloride)	79-00-5	1.60e-05	US EPA, 2018	Hepatic	Hepatocellular carcinoma	-10.8	-12.7
1,1,2-Trichloroethane (Vinyl trichloride)	79-00-5	1.60e-05	OEHHA, 2019	Digestive/Gastrointestinal	Hepatocellular carcinoma tumor	-10.8	-12.7
Trichloroethylene	79-01-6	4.10e-06	US EPA, 2018	Hematologic, Hepatic, Urinary	Renal cell carcinoma, non-Hodgkin's lymphoma, and liver tumors	-12.1	-14.1
Trichloroethylene	79-01-6	1.00e-06	ANSES, 2019	Kidney	Renal carcinoma	-13.5	-15.5
Trichloroethylene	79-01-6	2.00e-06	OEHHA, 2019	Digestive/Gastrointestinal, Respiratory, Hematologic	Hepatocellular adenoma and carcinoma, lung adenocarcinoma and malignant lymphoma	-12.8	-14.8
Ethyl carbamate (urethane)	51-79-6	2.90e-04	US EPA, 2018	Respiratory	Lung tumor	-7.87	-9.79
Ethyl carbamate (urethane)	51-79-6	2.90e-04	OEHHA, 2019	Respiratory	Lung tumor	-7.87	-9.79
Vinyl chloride (Chloroethylene)	75-01-4	3.80e-06	ANSES, 2019	Hepatic	Hepatic angiosarcomas and hepatocellular carcinomas	-12.2	-14.1
Vinyl chloride (Chloroethylene)	75-01-4	8.80e-06	US EPA, 2018	Hepatic	Liver angiosarcomas, angiomas, hepatomas, and neoplastic nodules	-11.4	-13.3
Vinyl chloride (Chloroethylene)	75-01-4	7.80e-05	OEHHA, 2019	Respiratory	Lung tumor	-9.18	-11.1
1,2-Diphenylhydrazine	122-66-7	2.20e-04	US EPA, 2018	Hepatic	Hepatocellular carcinomas and neoplastic liver nodules	-8.15	-10.1
1,3-Dichloropropene	542-75-6	4.00e-06	US EPA, 2018	Respiratory	Bronchioalveolar adenoma	-12.2	-14.1
2,4/2,6-Toluene diisocyanate mixture (TDI)	26471-62-5	1.10e-05	US EPA, 2018	Musculoskeletal	Subcutaneous fibroma/fibrosarcoma tumor	-11.1	-13.1
2-Nitropropane	79-46-9	5.60e-06	US EPA, 2018	Hepatic	Multiple hepatocellular carcinomas	-11.8	-13.7
4-Vinyl-1-cyclohexene	100-40-3	3.80e-06	ANSES, 2019	Reproductive	Granulosa ovary tumor and ovarian carcinoma	-12.2	-14.1
Bromoform	75-25-2	1.10e-06	US EPA, 2018	Gastrointestinal	Neoplastic lesions in the large intestine	-13.5	-15.4
Chlordane	57-74-9	1.00e-04	US EPA, 2018	Hepatic	Hepatocellular carcinoma	-8.94	-10.9
Chlorobenzilate	510-15-6	7.80e-05	US EPA, 2018	Hepatic	Liver tumor	-9.19	-11.1
Chloroprene	126-99-8	3.00e-04	US EPA, 2018	Reproductive, Ocular, Other, Hepatic, Gastrointestinal, Respiratory, Dermal	Alveolar/ bronchiolar adenoma or carcinoma hemangioma/ hemangiosarcoma (all organs), mammary gland adenocarcinoma, carcinoma, or adenoacanthoma forestomach squamous cell papilloma or carcinoma hepatocellular adenoma or carcinoma Harderian gland adenoma or carcinoma skin sarcoma and Zymbal's gland carcinoma	-7.84	-9.76
Heptachlor	76-44-8	1.30e-03	US EPA, 2018	Hepatic	Hepatocellular carcinomas	-6.38	-8.29
Hexachlorobutadiene	87-68-3	2.20e-05	US EPA, 2018	Urinary	Renal tubular adenomas and adenocarcinomas	-10.5	-12.4
Isopropyl Ether	108-20-3	2.20e-06	ANSES, 2019	Hematologic	Lymphoreticular tumor	-12.8	-14.7
Nitrobenzene	98-95-3	4.00e-05	US EPA, 2018	Hepatic, Urinary, Endocrine	Liver hepatocellular adenomas or carcinomas, kidney tubular adenomas or carcinomas, thyroid follicular cell adenomas or carcinomas	-9.86	-11.8
o-Toluidine	95-53-4	5.10e-05	US EPA, 2018	Other	Hemangiosarcomas	-9.61	-11.5
Tertiary butyl-acetate	540-88-5	1.30e-06	OEHHA, 2019	Kidney	Kidney	-13.3	-15.2
Toxaphene	8001-35-2	3.20e-04	US EPA, 2018	Hepatic	Hepatocellular carcinomas and neoplastic nodules	-7.78	-9.7
Vinyl bromide	593-60-2	3.20e-05	US EPA, 2018	Hepatic	Liver tumor	-10.1	-12

Note: IUR: inhalation unit risk; μ_{log}: natural logarithm mean value of the product $\alpha \times z$; σ_{log} natural logarithm standard deviation value of the product $\alpha \times z$;

lifetime exposure: 24 hours/day, 365 days/year for 70 years; occupational exposure: 8 hours/day, 250 days/year for 45 years. CSF values can be calculated

using the following formula: $CSF\ (kg.day/mg) = IUR\ (m^3/\mu g) \times 3{,}500)$.

3.3.2 Cancer risk for inhalation exposures

Fig. 5 presents a user guide for estimating the cancer risk for inhalation exposures following the proposed CRI approach, which consists of three main steps.

Step 1 – Selection of the chemical of interest

Select the chemical of interest from Table 5.

Example : benzene

Substance	Chemical abstract number	IUR (m³/µg)	Source	IUR establishment: cancer information		Product $\alpha \times z$	
				Tumor site	Tumor type	Lifetime: μ_{log} (m³/µg)	Occupational: μ_{log} (m³/µg)
…	…	…	…	…	…	…	…
Benzene	71-43-2	2.90e-05	OEHHA, 2019	Hematologic	Leukemia	-10.2	-12.1
Benzene	71-43-2	2.60e-05	ANSES, 2019	Hematologic	Leukemia	-10.3	-12.2
Benzene	71-43-2	7.80e-06	US EPA, 2018	Hematologic	Leukemia	-11.5	-13.4
…	…	…	…	…	…	…	…

Step 2 – Selection of the exposure setting

- If the exposure setting is given in Table 5

Retrieve the μ_{log} parameter of the $\alpha \times z$ for the chosen exposure setting.

Example: benzene with the IUR from OEHHA and environmental exposure

$\mu_{log} = -10.2$ and $\sigma_{log} = 0.42$

- If the exposure setting is not given in Table 5

Calculate the corresponding μ_{log} by multiplying the cancer IUR of the considered chemical by the exposure setting and by the z lognormal distribution of parameters $\mu_{log} = 0.27$ and $\sigma_{log} = 0.42$.

Example: population exposed to benzene for 12 hours a day, 7 days a week, 365 days a year for 70 years using the IUR from OEHHA

$$\alpha \times z = cancer\ IUR_{benzene} \times \frac{12}{24} \times \frac{365}{365} \times \frac{70}{70} \times z$$
$$= 2.9 \times 10^{-5} \times \frac{12}{24} \times \frac{365}{365} \times \frac{70}{70} \times Log - \mathcal{N}(0.27, 0.42)$$
$$= Log - \mathcal{N}(-10.9, 0.42)$$

→ $\mu_{log} = -10.9$ and $\sigma_{log} = 0.42$

Step 3 – Calculation of the risk distribution

Multiply the $\alpha \times z$ parameters from Step 2 by the airborne concentration distribution of a pollutant to obtain the risk distribution.

Fig. 5: User guide for estimating the cancer risk for inhalation exposures

For the sake of illustrating how to use our approach, let us choose the BaP cancer IUR from the OEHHA and consider that the airborne BaP concentration distribution remains constant over time and follows a lognormal distribution with parameters GM = 0.15 µg/m³ and GSD = 4. To calculate the CRI distribution, the concentration distribution was multiplied by the $\alpha \times z$ distribution of the

parameters provided in Table 5, with $\sigma_{log} = 0.42$ and $\mu_{log} = -6.54$ for lifetime exposure and $\mu_{log} = -8.46$ for occupational exposure. Table 6 presents the results of the CRI and all existing cancer risk indicators for the risk (corresponding to the 90th percentile of the risk distribution) of lung cancer following the particular exposure settings and the probability (likelihood) of obtaining a $1/10^6$, $1/10^5$, $1/10^4$, or $1/10^3$ chance of observing one additional lung cancer case over the given period of exposure. Regardless of the exposure setting considered, existing indicators gave different risks. The CRI always gave the second highest risk, which was two times lower than the risk given by ILCR4 and 2.2, 2.2, 12, 16, 36, 111 and $2x10^{11}$ times higher than the risks given by indicators LCR, RC, RM, ILCR3, ILCR5, ILCR2 and ILCR1, respectively.

Table 6: Comparison of the risk of lung cancer and the probability of different levels of risk obtained with the different cancer risk indicators following lifetime and occupational BaP exposure

Exposure setting	Risk estimate	CRI	*ILCR1*	*ILCR2*	*ILCR3*	*ILCR4*	*ILCR5*	*LCR*	*RC*	*RM*
Occupational	P_{90} risk	**3.1×10^{-4}**	1.4×10^{-15}	2.8×10^{-6}	1.9×10^{-5}	6.3×10^{-4}	8.7×10^{-6}	1.4×10^{-4}	1.4×10^{-4}	2.5×10^{-5}
	$L\ 10^{-6}$	**0.99**	0	0.22	0.69	1	0.55	0.98	0.98	0.73
	$L\ 10^{-5}$	**0.84**	0	0.02	0.14	0.94	0.10	0.74	0.74	0.22
	$L\ 10^{-4}$	**0.31**	0	0	0	0.46	0	0.16	0.16	0
	$L\ 10^{-3}$	**0.02**	0	0	0	0.08	0	0	0	0
Lifetime	P_{90} risk	**2.1×10^{-3}**	9.8×10^{-15}	1.9×10^{-5}	1.3×10^{-4}	4.3×10^{-3}	5.9×10^{-5}	9.5×10^{-4}	9.5×10^{-4}	1.7×10^{-4}
	$L\ 10^{-6}$	**0.99**	0	0.69	0.97	1	0.91	1	1	0.98
	$L\ 10^{-5}$	**0.98**	0	0.14	0.73	0.99	0.43	0.98	0.98	0.78
	$L\ 10^{-4}$	**0.78**	0	0	0.14	0.86	0.06	0.64	0.64	0.19
	$L\ 10^{-3}$	**0.19**	0	0	0	0.33	0	0.10	0.10	0

Note: CRI: consensus risk indicator; P_{90}: 90th percentile of the risk distribution for lung cancer following a given exposure setting; $L\ 10^{-6}$, $L\ 10^{-5}$, $L\ 10^{-4}$, and $L\ 10^{-3}$: probability (likelihood) of obtaining a $1/10^6$, $1/10^5$, $1/10^4$, or $1/10^3$ chance of observing one additional case of lung cancer over a given period of exposure to airborne BaP concentration following a lognormal distribution with parameters GM = 0.15 µg/m^3 and GSD = 4. Lifetime exposure: 24 hours/day, 365 days/year for 70 years; occupational exposure: 8 hours/day, 250 days/year for 45 years.

Fig. 6 shows a screenshot of the Shiny web application (InCaRisk) created to implementthe CRI approach for cancer risk estimation following inhalation exposure. InCaRisk provides different options for cancer risk estimation. Beyond making the risk estimation easier, this app offers the chance to have an immediate glimpse into the results and to see how the results change according to different setting configurations. It is possible to choose any of the 199 substances, choose the IUR of a given institution, upload a file containing concentration distributions, configure the exposure settings and display any of the eight existing cancer risk indicators (Table 1) for comparison with the CRI. The resulting cancer estimates are immediately available and can be seen in interactive easy-to-read graphs, which are downloadable (link to access the web app: https://exporisk-timc.imag.fr/InCaRisk/).

InCaRisk: Inhalation Cancer Risk estimation

Pascal Petit, Anne Maître & Dominique J. Bicout

Chemical of interest

Source
OEHHA

Chemical
Benzene

Airborne concentration distribution setting

Geometric mean
1 — 150 — 1,000
1 100.9 200.8 300.7 400.6 500.5 600.4 700.3 800.2 900.1 1,000

Concentration unit
µg/m3

Geometric standard deviation
1 — 4 — 20
1 2.9 4.8 6.7 8.6 10.5 12.4 14.3 16.2 18.1 20

Number of iterations
10000

Change in concentration/year
-1,000 — 0 — 1,000
-1,000 -800 -600 -400 -200 0 200 400 600 800 1,000

Concentration unit
ng/m3

Upload a concentration file
Browse... No file selected

Header
● True
○ False

Decimal
● Comma
○ Period

Exposure setting

Number of hours of per day
0 — 8 — 24
0 3 6 9 12 15 18 21 24

Number of days per year
0 — 250 — 366
0 37 74 111 148 185 222 259 296 333 366

Number of years
0 — 45 — 100
0 10 20 30 40 50 60 70 80 90 100

Population exposed
1 — 10

x 10^
4

Cancer risk indicator(s) to display

☐ ILCR1 ☐ ILCR2 ☑ ILCR3 ☑ ILCR4 ☐ ILCR5 ☐ LCR ☐ RC ☐ RM

Number of visits

10

Cancer type: Leukemia
Cancer site: Hematologic
Cancer risk from CRI: 0.00818 [2.35e-05 - 0.0284] (90% [2.5% - 97.5%])

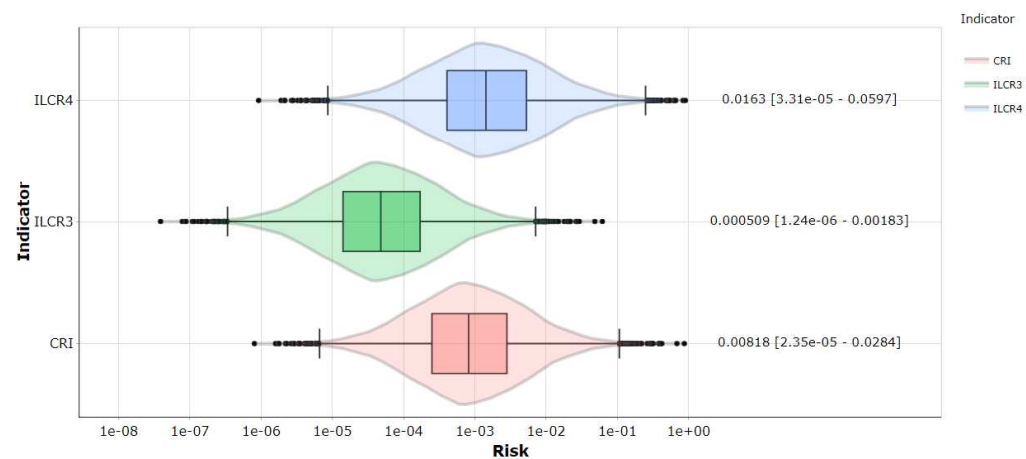| Risk | Cases | Data source | News | Help | Mentions légales |
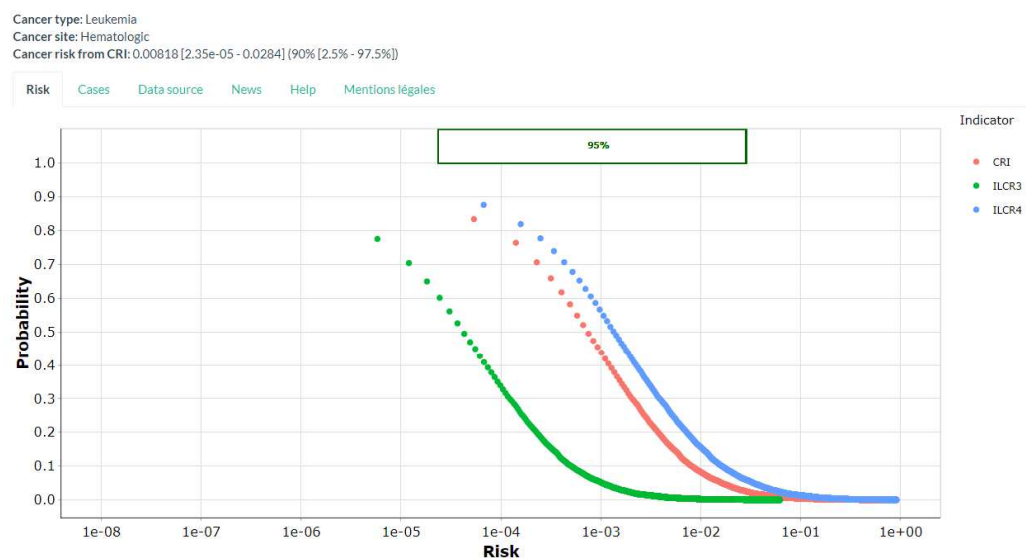
Fig.1: Probability of exceeding a risk

Fig.2: Distribution of the estimated cancer risk

Please cite: Petit P, Maître A, Bicout D. A consensus approach for estimating health risk: application to inhalation cancer risks. 2020. Submitted to Environ Res. Access

36

Fig. 6: Screenshot of the Shiny web application InCaRisk for cancer risk estimation using the CRI following inhalation exposure (https://exporisk-timc.imag.fr/InCaRisk/)

4. DISCUSSION

The goal of this work was to propose a structured and pragmatic approach for creating a consensus distribution, given a specific route of exposure and health outcome/event, and demonstrate its feasibility and easy implementation in conducting health risk assessment. We illustrated the practical side, ease of implementation and effectiveness of our approach on human cancer risk assessment for inhalation exposure.

4.1 Advantages of the proposed consensus approach

When assessing health risk, a reference value (e.g., IUR, CSF, MRL depending on the risk considered) is always used. However, these values do not provide a range (e.g., 95% confidence interval) for considering possible uncertainties and errors, which can be misleading and could lead to incorrect decisions (Slob et al., 2014; Du et al., 2014). The $\alpha \times z$ provided in this study is an effective IUR that has a distribution contrary to that of the "classical" IUR, which is only expressed as a single value. Providing a distribution (and thus an uncertainty range) instead of a single value is preferable and can help in determining whether the knowledge regarding a health risk is poor and to improve the reliability of the risk estimation (Bokkers et al., 2017).

Existing risk indicators give results with vastly different levels of risk (Petit et al., 2019) because the approaches differ between countries and organizations and because there is no international "gold standard" (Abt et al., 2010; Chartres et al., 2019; Slob et al., 2014). This is problematic because depending on the chosen indicator, the decisions made will be completely different, which could be misleading. Our approach addresses this issue by providing a single result that can be adapted to any exposure conditions that are judged legitimate, as illustrated through both lifetime and occupational exposures to BaP. In addition, our approach is based on similar principles for all types of chemicals, which can help in avoid inconsistencies between studies and countries (Rotter et al., 2018). It is important to note that while our approach provides a single result, the interpretation of the estimated risk will still be managed differently by different organizations that have different jurisdictions and regulatory settings. This could lead to discrepancies and conflicting conclusions between organizations and countries. For instance, a theoretical increased risk of cancer for 1 in a million is considered

unacceptable by the US EPA, a theoretical increased risk of cancer for 1 in 10,000 is considered the maximal risk level in the European Union, and a theoretical increased risk of cancer for 1 in 1,000 is considered a high priority by the US EPA and determined to be a significant risk level by the US Supreme Court (Petit et al., 2019).

To aid the wider implementation of the CRI approach, a user-friendly and interactive web application, called InCaRisk, was created. Beyond making risk estimation easier, this app offers the chance to have an immediate glimpse of the results to see how they change according to different setting configurations. The resulting cancer estimates are immediately available and can be seen in easily-readable and interactive graphs. This can be more useful and informative when conducting a health risk assessment than using only one single indicator, as InCaRisk can provide consistency and supports direct comparisons of risk indicators, studies and countries. Additionally, InCaRisk provides the ability to assess changes in risk. Periodic updates of the InCaRisk will allow for the integration of updated and new data regarding existing risk indicators and reference values as well as new functionalities.

Finally, our approach is not limited to inhalation cancer risk estimation. Indeed, it can be used to estimate other functional forms of risk and to study other routes of exposure and other toxic effects, and it can be used with other indicators of the same class (e.g., inhalation cancer risk indicators). CRI could also be adapted and used for deterministic risk (e.g., hazard ratios) and can be applied in other fields, contexts and studies involving similar problems such as problems in which the construction of a consensus distribution is needed/useful. In the future, we plan to conduct the same work for other routes of exposure for cancer risk, for non-cancer risks and to address the question of co-exposure/multi-exposure.

4.2 Limitations of this study

Values of the product $\alpha \times z$ reported in Table 5 were determined using reference values (IURs and CSFs) from the OEHHA (2019), US EPA (2018) and ANSES (2019). If these values are updated or if reference values established by other institutions are used, the product $\alpha \times z$ may be different (only the term α would change) for a given substance, as reference values usually differ between institutions

because organizations do not necessarily use the same methodology and studies to establish them (Tables 5 and A.1). For instance, cancer IUR and CSF values from the OEHHA (2019), US EPA (2018) and ANSES (2019) are established mostly using tumor incidence data from animal studies for lifetime exposure (70 years) and for different types of cancer and tumorigenesis mechanisms depending on the substance considered (Tables 5 and A.1). The choice of the most relevant or legitimate IUR to use is the responsibility of the person conducting the assessment.

In addition, we assumed that the exposure conditions remained constant throughout time, which is not necessarily true in reality; levels can vary over time depending on many factors, such as meteorological conditions, changes in industrial processes, mobility or individual factors (e.g., age, genetic susceptibility, and preexisting disease) (Ansari and Ehrampoush, 2019; Creely et al., 2007; Shen et al., 2014; Song et al., 2019; Vu et al., 2013; Wang et al., 2019).

The construction of the CRI was based on the linear aggregation of the probability distribution of indicators, using the overlapping areas between an individual indicator's distribution and an aggregated reference distribution for the assignment of weight. There are other ways to assign weights for aggregation purposes, such as ranking methods, setting equal weights or the natural-conjugate method (Clemen and Winkler, 1999; Jacobs, 1995; Liu et al., 2012; McBride and Varkoi, 2014; Winkler, 1968; Winkler and Cummings, 1972). Using another weight assignment method would result in a different CRI. The advantage of using the overlap in the assignment of weights is that the overlapping area of the PDFs contains more information than the other aforementioned techniques (Liu et al., 2012).

The construction of the CRI is also dependent on the number of indicators used and on the different parameters that have to be chosen to determine the weights (Eq. 1 to 9). We kept all eight cancer risk indicators in the consensus analysis because we had no approach to rate them and because we assumed that they each hold an element of truth. The eight cancer risk indicators used in this study were found through a literature search conducted in a previous work (Petit et al., 2019). As this was only a literature search and not a systematic review, other cancer risk indicators for inhalation exposure may have been missed. If new cancer risk indicators were to be found, it is quite straightforward to integrate them in the construction of the CRI and update the InCaRisk app.

To create the CRI, we chose to use the 90th percentile as a statistic (s parameter in Eq. 9). Choosing another statistic would yield different results. To determine offset parameter b (Eq. 9), we chose the equidistant point (50%) between s_r and $\max(s_i)$. By doing so, we favored risk indicators that are more protective. To favor risk indicators that are less protective, the equidistant point (50%, $\theta = 0.5$) between s_r and $\min(s_i)$ could be used. Various other combinations are also possible depending on the goal that one wants to achieve.

In this work, we applied our approach to the inhalation cancer risk. However, risk assessment is not only about one kind of risk, such as cancer, one type of route of exposure (e.g., inhalation) or one source of exposure (e.g., BaP) (Kienzler et al., 2016; Lentz et al., 2015). In reality, people are simultaneously exposed to a broad range of chemicals and other stressors from various sources (occupational and non-occupational). The proposed approach can only be used for one type of risk/health outcome, one route of exposure and one source of exposure. However, the issue of multi-exposure will be addressed in the future.

4.3 Conclusion

In conclusion, the consensus approach presented in this manuscript can be useful for quantifying the health risk of individuals exposed to a given substance, as it could add value to exposure risk characterization by comprehensively considering several risk indicators. The proposed approach integrates several cancer risk indicators to derive a "final" cancer risk assessment result using overlapping areas to combine risk distributions into a single consensus risk distribution. The proposed approach could thus be useful for risk managers, practitioners, and decision makers by providing consistency and supporting direct comparisons between studies and countries to help in the establishment of appropriate safe pollutant guidelines. The proposed approach could facilitate and enhance the quality of regulatory decisions and the protection of populations exposed to environmental pollutants.

Author contributions

Pascal Petit: Conceptualization, Methodology, Software, Formal analysis, Investigation, Data Curation, Writing - Original Draft, Visualization. **Dominique J. Bicout**: Conceptualization,

Methodology, Validation, Writing - Review & Editing, Supervision. **Anne Maître**: Writing - Review & Editing.

Declaration of interests: The authors declare that they have no known competing financial interests or personal relationships that could have appeared to influence the work reported in this paper.

REFERENCES

Abt, E., Rodricks, J.V., Levy, J.I., Zeise, L., Burke, T.A., 2010. Science and decisions: advancing risk assessment. **Risk. Anal.** 30, 1028-1036. https://doi.org/10.1111/j.1539-6924.2010.01426.x.

Allan, M., Jones-Otazo, H., Richardson, G.M., 2009. Inhalation Rates for Risk Assessments Involving Construction Workers in Canada. **Hum. Ecol. Risk. Assess.** 15(2), 371-387. https://doi.org/10.1080/10807030902761445.

Allan, M., Richardson, G.M., 1998. Probability Density Functions Describing 24-Hour Inhalation Rates for Use in Human Health Risk Assessments. **Hum. Ecol. Risk. Assess.** 4(2), 379-408. https://doi.org/10.1080/10807039891284389.

Amarillo, A.C., Tavera Busso, I., Carreras, H., 2014. Exposure to polycyclic aromatic hydrocarbons in urban environments: health risk assessment by age groups. **Environ. Pollut.** 195, 157-162. https://doi.org/10.1016/j.envpol.2014.08.027.

Ansari, M., Ehrampoush, M.H., 2019. Meteorological correlates and AirQ + health risk assessment of ambient fine particulate matter in Tehran, Iran. **Environ. Res.** 170, 141-150. https://doi.org/10.1016/j.envres.2018.11.046.

ANSES (French Agency for Food, Environmental and Occupational Health & Safety), 2019. List of toxicity reference values (TRVs) established by ANSES. ANSES, Maisons-Alfort (France). [last accessed 06 February 2019]. Available from: https://www.anses.fr/en/content/list-toxicity-reference-values-trvs-established-anses.

ATSDR (Agency for Toxic Substances and Disease Registry), 2005. Public health assessment guidance manual (update). Agency for Toxic Substances and Disease Registry. ATSDR, Atlanta (USA). [last accessed 11 July 2020]. Available from: http://www.atsdr.cdc.gov/hac/PHAManual/PDFs/PHAGM_final1-27-05.pdf.

Backhaus, T., Faust, M., 2012. Predictive environmental risk assessment of chemical mixtures: a conceptual framework. **Environ. Sci. Technol.** 46(5), 2564-2573. https://doi.org/10.1021/es2034125.

Bokkers, B.G.H., Mengelers, M.J., Bakker, M.I., Chiu, W.A., Slob, W. 2017. APROBA-Plus: A probabilistic tool to evaluate and express uncertainty in hazard characterization and exposure assessment of substances. **Food. Chem. Toxicol.** 110, 408-417. https://doi.org/10.1016/j.fct.2017.10.038.

Buonanno, G., Giovinco, G., Morawska, L., Stabile, L., 2015. Lung cancer risk of airborne particles for Italian population. **Environ. Res.** 142, 443-451. https://doi.org/10.1016/j.envres.2015.07.019.

Callén, M.S., Iturmendi, A., Lopez, J.M., 2014. Source apportionment of atmospheric PM2.5-bound polycyclic aromatic hydrocarbons by a PMF receptor model. Assessment of potential risk for human health. **Environ. Pollut.** 195, 167-177. https://doi.org/10.1016/j.envpol.2014.08.025.

Chang, W., Cheng, J., Allaire, J., Xie, Y., McPherson, J., 2018. Shiny: Web Application Framework for R. R package version 1.4.0.

Chartres, N., Bero, L.A., Norris, S.L., 2019. A review of methods used for hazard identification and risk assessment of environmental hazards. **Environ. Int.** 123, 231-239. https://doi.org/10.1016/j.envint.2018.11.060.

Chen, S.C., Liao, C.M., 2006. Health risk assessment on human exposed to environmental polycyclic aromatic hydrocarbons pollution sources. **Sci. Total. Environ.** 366, 112-123. https://doi.org/10.1016/j.scitotenv.2005.08.047.

Clemen, R.T., Winkler, R.L., 1999. Combining Probability Distributions From Experts in Risk Analysis. **Risk. Anal.** 19, 187-203. https://doi.org/10.1111/j.1539-6924.1999.tb00399.x.

Creely, K.S., Cowie, H., Van Tongeren, M., Kromhout, H., Tickner, J., Cherrie, J.W., 2007. Trends in inhalation exposure--a review of the data in the published scientific literature. **Ann. Occup. Hyg.** 51, 665-678. https://doi.org/10.1093/annhyg/mem050.

Cuadras, A., Rovira, E., Marcé, R.M., Borrull, F., 2016. Lung cancer risk by polycyclic aromatic hydrocarbons in a Mediterranean industrialized area. **Environ. Sci. Pollut. Res. Int.** 23(22), 23215-23227. https://doi.org/10.1007/s11356-016-7566-4.

Du, Z., Mo, J., Zhang, Y., 2014. Risk assessment of population inhalation exposure to volatile organic compounds and carbonyls in urban China. **Environ. Int.** 73, 33–45. https://doi.org/10.1016/j.envint.2014.06.014.

Hoseini, M., Yunesian, M., Nabizadeh, R., Yaghmaeian, K., Ahmadkhaniha, R., Rastkari, N., et al., 2016. Characterization and risk assessment of polycyclic aromatic hydrocarbons (PAHs) in urban atmospheric Particulate of Tehran, Iran. **Environ. Sci. Pollut. Res. Int.** 23, 1820-1832. https://doi.org/10.1007/s11356-015-5355-0.

Hsu, H.I., Lin, M.Y., Chen, Y.C., Chen, W.Y., Yoon, C., Chen, M.R., et al., 2014. An integrated approach to assess exposure and health-risk from polycyclic aromatic hydrocarbons (PAHs) in a fastener manufacturing industry. **Int. J. Environ. Res. Public. Health.** 11, 9578-9594. https://doi.org/10.3390/ijerph110909578.

Hu, Y., Bai, Z., Zhang, L., Wang, X., Zhang, L., Yu, Q., et al., 2007. Health risk assessment for traffic policemen exposed to polycyclic aromatic hydrocarbons (PAHs) in Tianjin, China. **Sci. Total. Environ.** 382, 240-250. https://doi.org/10.1016/j.scitotenv.2007.04.038.

Huang, H.F., Xing, X.L., Zhang, Z.Z., Qi, S.H., Yang, D., Yuen, D.A., et al., 2016. Polycyclic aromatic hydrocarbons (PAHs) in multimedia environment of Heshan coal district, Guangxi: distribution, source diagnosis and health risk assessment. **Environ. Geochem. Health.** 38, 1169-1181. https://doi.org/10.1007/s10653-015-9781-1.

Irvine, G..M, Blais, J.M., Doyle, J.R., Kimpe, L.E., White, P.A., 2014. Cancer risk to First Nations' people from exposure to polycyclic aromatic hydrocarbons near in-situ bitumen extraction in Cold Lake, Alberta. **Environ. Health.** 13, 7. https://doi.org/10.1186/1476-069X-13-7.

Jacobs, R.A., 1995. Methods for combining experts' probability assessments. **Neural. Comput.** 7(5), 867-888. https://doi.org/10.1162/neco.1995.7.5.867.

Jia, Y., Stone, D., Wang, W., Schrlau, J., Tao, S., Simonich, S.L., 2011. Estimated reduction in cancer risk due to PAH exposures if source control measures during the 2008 Beijing Olympics were sustained. **Environ. Health. Perspect.** 119, 815-820. https://doi.org/10.1289/ehp.1003100.

Kienzler, A., Bopp, S.K., van der Linden, S., Berggren, E., Worth, A., 2016. Regulatory assessment of chemical mixtures: Requirements, current approaches and future perspectives. **Regul. Toxicol. Pharmacol.** 80, 321-334. https://doi.org/10.1016/j.yrtph.2016.05.020.

Korobitsyn, B.A., 2011. Multiplicative model for assessment of chemical-induced cancer risk. **Int. J. Environ. Health. Res.** 21(1), 1-21. https://doi.org/10.1080/09603123.2010.499454.

Lebret, E., 2015. Integrated Environmental Health Impact Assessment for Risk Governance Purposes; Across What Do We Integrate? **Int. J. Environ. Res. Public. Health.** 13(1), ijerph13010071. https://doi.org/10.3390/ijerph13010071.

Lentz, T.J., Dotson, G.S., Williams, P.R., Maier, A., Gadagbui, B., Pandalai, S.P., et al., 2015. Aggregate Exposure and Cumulative Risk Assessment--Integrating Occupational and Non-occupational Risk Factors. **J. Occup. Environ. Hyg.** 12, S112-126. https://doi.org/10.1080/15459624.2015.1060326.

Li, P.H., Kong, S.F., Geng, C.M., Han, B., Lu, B., Sun, R.F., et al., 2013. Health risk assessment for vehicle inspection workers exposed to airborne polycyclic aromatic hydrocarbons (PAHs) in their work place. **Environ. Sci. Process. Impacts.** 15, 623-632. https://doi.org/10.1039/C2EM30708A.

Li, H., Zeng, X., Zhang, D., Chen, P., Yu, Z., Sheng, G., et al., 2014. Occurrence and carcinogenic potential of airborne polycyclic aromatic hydrocarbons in some large-scale enclosed/semi-enclosed vehicle parking areas. **J. Hazard. Mater.** 274, 279-286. https://doi.org/10.1016/j.jhazmat.2014.04.016.

Lin, Y.C., Lee, W.J., Chen, S.J., Chang-Chien, G.P., Tsai, P.J., 2008. Characterization of PAHs exposure in workplace atmospheres of a sinter plant and health-risk assessment for sintering workers. **J. Hazard. Mater.** 158, 636-643. https://doi.org/10.1016/j.jhazmat.2008.02.006.

Liu, H.H., Yang, H.H., Chou, C.D., Lin, M.H., Chen, H.L., 2010. Risk assessment of gaseous/particulate phase PAH exposure in foundry industry. **J. Hazard. Mater.** 181, 105-111. https://doi.org/10.1016/j.jhazmat.2010.04.097.

Liu, X., Ghorpade, A., Tu, Y.L., Zhang, W.J., 2012. A novel approach to probability distribution aggregation. **Inform. Sci.** 188, 269-275. https://doi.org/10.1016/j.ins.2011.11.002.

McBride, T., Varkoi, T., 2014. A method for aggregating ordinal process assessment measures. **J. Softw. Evol. Process.** 26(12), 1267-1279. https://doi.org/10.1002/smr.1676.

Mesnage, R., Antoniou, M.N., 2017. Facts and Fallacies in the Debate on Glyphosate Toxicity. **Front. Public. Health.** 5, 36. https://doi.org/10.3389/fpubh.2017.00316.

OEHHA (California Office of Environmental Health Hazard Assessment), 2019. Consolidated table of OEHHA/ARB approved risk assessment health values. OEHHA, Sacramento (USA). [last accessed 06 February 2019]. Available from: https://ww3.arb.ca.gov/toxics/healthval/contable.pdf.

Park, R.M., 2018. Risk assessment for metalworking fluids and cancer outcomes. **Am. J. Ind. Med.** 61(3), 198-203. https://doi.org/10.1002/ajim.22809.

Petit, P., Maître, A., Persoons, R., Bicout, D.J., 2019. Lung cancer risk assessment for workers exposed to polycyclic aromatic hydrocarbons in various industries. **Environ. Int.** 124, 109-120. https://doi.org/10.1016/j.envint.2018.12.058.

Qu, C., Li, B., Wu, H., Wang, S., Giesy, J.P., 2015. Multi-pathway assessment of human health risk posed by polycyclic aromatic hydrocarbons. **Environ. Geochem. Health.** 37, 587-601. https://doi.org/10.1007/s10653-014-9675-7.

Ramirez, N., Cuadras, A., Rovira, E., Marce, R.M., Borrull, F., 2011. Risk assessment related to atmospheric polycyclic aromatic hydrocarbons in gas and particle phases near industrial sites. **Environ. Health. Perspect.** 119, 1110-1116. https://doi.org/10.1289/ehp.1002855.

Rhomberg, L.R., Mayfield, D.B., Prueitt, R.L., Rice, J.W., 2018. A bounding quantitative cancer risk assessment for occupational exposures to asphalt emissions during road paving operations. **Crit. Rev. Toxicol.** 48(9), 713-737. https://doi.org/10.1080/10408444.2018.1528208.

Rotter, S., Beronius, A., Boobis, A.R., Hanberg, A., van Klaveren, J., Luijten, M. et al., 2018. Overview on legislation and scientific approaches for risk assessment of combined exposure to multiple chemicals: the potential EuroMix contribution. **Crit. Rev. Toxicol.** 48(9), 796-814. https://doi.org/10.1080/10408444.2018.1541964.

Shen, H., Tao, S., Liu, J., Huang, Y., Chen, H., Li, W., et al., 2014. Global lung cancer risk from PAH exposure highly depends on emission sources and individual susceptibility. **Sci. Rep.** 4, 6561. https://doi.org/10.1038/srep06561.

Singh, A., Kesavachandran, C.N., Kamal, R., Bihari, V., Gupta, M.K., Mudiam, M.K., et al., 2016. Assessing hazardous risks of indoor airborne polycyclic aromatic hydrocarbons in the kitchen and its association with lung functions and urinary PAH metabolites in kitchen workers. **Clin. Chim. Acta.** 452, 204-213. https://doi.org/10.1016/j.cca.2015.11.020.

Slob, W., Bakker, M.I., Biesebeek, J.D., Bokkers, B.G., 2014. Exploring the uncertainties in cancer risk assessment using the integrated probabilistic risk assessment (IPRA) approach. **Risk. Anal.** 34, 1401-1422. https://doi.org/10.1111/risa.12194.

Soltani, N., Keshavarzi, B., Moore, F., Tavakol, T., Lahijanzadeh, A.R., Jaafazadeh, N., et al., 2015. Ecological and human health hazards of heavy metals and polycyclic aromatic hydrocarbons (PAHs) in road dust of Isfahan metropolis, Iran. **Sci. Total. Environ.** 505, 712-723. https://doi.org/10.1016/j.scitotenv.2014.09.097.

Song, Y., Huang, B., He, Q., Chen, B., Wei, J., Mahmood, R., 2019. Dynamic assessment of PM 2.5 exposure and health risk using remote sensing and geo-spatial big data. **Environ. Pollut.** 253, 288-296. https://doi.org/10.1016/j.envpol.2019.06.057.

Tanguy, J., Zeghnoun, A., Dor, F., 2007. Description du poids corporel en fonction du sexe et de l'âge dans la population française. **Environnement, Risques & Santé.** 6(3), 179-187. https://doi.org/10.1684/ers.2007.0084.

Tarazona, J.V., Court-Marques, D., Tiramani, M., Reich, H., Pfeil, R., Istace, F. et al., 2017. Glyphosate toxicity and carcinogenicity: a review of the scientific basis of the European Union assessment and its differences with IARC. **Arch. Toxicol.** 91(8), 2723-2743. https://doi.org/10.1007/s00204-017-2032-8.

US EPA (Environmental protection Agency), 2005. Guidelines for carcinogen risk assessment. 2005. EPA/630/P-03/001F. Risk Assessment Forum. US EPA, Washington (DC). [last accessed 15 July 2020]. Available from: http://www2.epa.gov/osa/guidelines-carcinogen-risk-assessment.

US EPA (Environmental Protection Agency), 2018. Table 1. Prioritized Chronic Dose-Response Values for Screening Risk Assessments. US EPA, Washington (DC). [last accessed 06 February 2019]. Available from: https://www.epa.gov/sites/production/files/2014-05/documents/table1.pdf.

US EPA (Environmental Protection Agency), 2019. Basic Information about the Integrated Risk Information System. US EPA, Washington (DC). [last accessed 14 January 2019]. Available from: https://www.epa.gov/iris/basic-information-about-integrated-risk-information-system.

Vu, V.H., Le, X.Q., Pham, N.H., Hens, L., 2013. Application of GIS and modelling in health risk assessment for urban road mobility. **Environ. Sci Pollut. Res. Int.** 20(8), 5138-5149. https://doi.org/10.1007/s11356-013-1492-5.

Wang, J., Chen, S., Tian, M., Zheng, X., Gonzales, L., Ohura, T., et al., 2012. Inhalation cancer risk associated with exposure to complex polycyclic aromatic hydrocarbon mixtures in an electronic waste and urban area in South China. **Environ. Sci. Technol.** 46, 9745-9752. https://doi.org/10.1021/es302272a.

Wang, Y., Hu, L., Lu, G., 2014. Health risk analysis of atmospheric polycyclic aromatic hydrocarbons in big cities of China. **Ecotoxicology.** 23, 584-588. https://doi.org/10.1007/s10646-014-1179-9.

Wang, N., Mengersen, K., Tong, S., Kimlin, M., Zhou, M., Wang, L., et al., 2019. Short-term association between ambient air pollution and lung cancer mortality. **Environ. Res.** 179(Pt A), 108748. https://doi.org/10.1016/j.envres.2019.108748.

Warner, G.R., Flaws, J.A., 2018. Bisphenol A and Phthalates: How Environmental Chemicals Are Reshaping Toxicology. **Toxicol. Sci.** 166(2), 246-249. https://doi.org/10.1093/toxsci/kfy232.

Williams, P.R., Dotson, G.S., Maier, A., 2012. Cumulative Risk Assessment (CRA): transforming the way we assess health risks. **Environ. Sci. Technol.** 46(20), 10868-10874. https://doi.org/10.1021/es3025353.

Winkler, R.L., 1968. The consensus of subjective probability distributions. **Manage. Sci.** 15, B-61-B-75. https://doi.org/10.1287/mnsc.15.2.B61.

Winkler, R.L., Cummings, L.L., 1972. On the choice of a consensus distribution in Bayesian analysis. **Organ. Behav. Hum. Perform.** 7, 63-76. https://doi.org/10.1016/0030-5073(72)90007-4.

Yu, Y., Li, Q., Wang, H., Wang, B., Wang, X., Ren, A., et al., 2015. Risk of human exposure to polycyclic aromatic hydrocarbons: A case study in Beijing, China. **Environ. Pollut.** 205, 70-77. https://doi.org/10.1016/j.envpol.2015.05.022.